PROBLEMS IN GEOPHYSICS FOR THE NEW MILLENNIUM
Eds.Enzo Boschi, Göran Ekström and Andrea Morelli

The late stage of retreating subduction in the Alpine-Mediterranean region: constraints from travel time seismic tomography

ANDREA MORELLI and CLAUDIA PIROMALLO
Istituto Nazionale di Geofisica, Roma, Italy

Abstract - Seismological modelling of the upper mantle of the Africa-Eurasia collision region has given images of its structure which can be used to supplement surface (geologic) information in the attempt to understand past and active tectonic processes. A foremost feature of the region is given by the sinuous Alpine-Mediterranean thrust belt, under which subducted lithosphere is imaged by seismic tomography as seismically fast material (colder than ambient rock). Several arcuate structures are present, combining an external thrust front with an internal extensional basin, originated by slab rollback: the Hellenic arc with the Aegean basin, the Calabrian arc with the Tyrrhenian Sea, the Betic-Rif with the Alboran Sea, and the Carpathians with the Pannonian basin. These systems are at different stages of their life, and all but the Hellenic-Aegean appear close to their terminal phase. Shape and extent of subducted slabs provide constraints on their evolution. Tomographic results, in all but the Hellenic-Aegean system, show a general lack of overall continuity of the subducted bodies, and in many cases support the idea that other processes, such as slab detachment or mantle delamination, contributed to shape the present day tectonics. Although tomographic results have steadily improved image resolution with time, differences between studies may lead to different interpretations. Better understanding of processes active at the late phases of subduction needs a close interplay between tomography, geology, and mantle dynamics calculations.

1 Introduction

The most evident geographic and geologic features of the European and Mediterranean area, marking the Alpine orogenic belt, are the result of convergent motion of the African and Eurasian plates. Convergence has existed since Mesozoic times, and involved the closure of the 3000 km wide Tethys ocean, first entailing subduction of oceanic crust and, later, continental collision (see, *e.g.*, Dercourt *et al.*, 1986; Le Pichon *et al.*, 1988; Dewey *et al.*, 1989). The change from a system dominated by subduction to one dominated by collision occurred between 100 and 80 Ma in the west, and gradually migrated to the east, where the impact

between India and Eurasia eventually closed the Neo-Tethys at about 35 Ma. At that time (Oligocene), overthrusting was a dominant process in the Mediterranean region (Figure 1, top), while extensional stresses were instead present in the Western European platform. Shortening stopped under the Alps at about 35-40 Ma (late Eocene – early Oligocene) (Royden and Burchfiel, 1989), while subduction of oceanic and thinned continental crust was instead continuing under the Carpathians arc. The line of suture between Africa and Eurasia developed a distinctive sinuosity as the subduction fronts retreated, while the two plates continued to converge (Şengör, 1993). During the late Miocene (Figure 1, center) the Tyrrhenian basin began opening as the Calabrian trench retreated, while continental lithosphere began to be subducted under the Carpathians. Opening of the Aegean followed later on, also as an extensional back-arc basin (Figure 1, bottom).

Some of the features of subduction in the Mediterranean are rather peculiar. Tight curvature arcuate belts, backed by internal basins characterized by recent subsidence, are a typical occurrence: the Hellenides and the Aegean basin; the Apennines-Calabrides and the Tyrrhenian basin; the Betic-Rif belts and the Alboran Sea; the Carpathians and the Pannonian basin (Figure 1, bottom). Subduction is (or has been) present with different timings under these arcs, currently ranging from well developed and active subduction slabs, as in the Hellenic arc, to the terminal phase of Carpathian subduction. Within this spectrum, a peculiar situation is that of the Calabrian arc, progressively retreated by outward arc migration, and now possibly facing a critical stage, strangled in the narrow gap between the African foreland and Adria (Malinverno and Ryan, 1986). Subduction, therefore, holds an important place in the geodynamics of the Euro-Mediterranean region.

Clear evidence leading to the inference of the existence of past and active subduction in the Mediterranean came first from geology. Paleogeographic reconstructions showed how large amounts of crust have disappeared from the surface and sunk into the mantle. The modern key tool for revealing the signature of geodynamic processes, now buried into the mantle, is seismic tomography. In this paper, we present and discuss results achieved by seismic tomography in mapping the structure of the upper mantle, and in contributing to the understanding of the geodynamic processes which shaped the lithosphere. A thorough examination and discussion of tomographic studies of the Euro-Mediterranean region would however easily fill a thick book. We concentrate on subduction processes. Because of the length limitation, we neglect technical details, as they can be found in the papers referenced. We most often refer to a newly developed tomographic model of the upper mantle of the Mediterranean area, PM0.5 (Piromallo and Morelli, 2000b). Only the features, that are relevant for the purpose of the present paper, will however be outlined in the following sections, and we will also omit most methodological details, to be found elsewhere (Piromallo and Morelli, 2000b).

Besides comparing the results of different tomographic studies, we also discuss how their features relate to proposed geodynamic models. Comparison of tomographic results with tectonic studies is useful to understand consequences of kinematic models; but also because the association yields a critical evaluation of

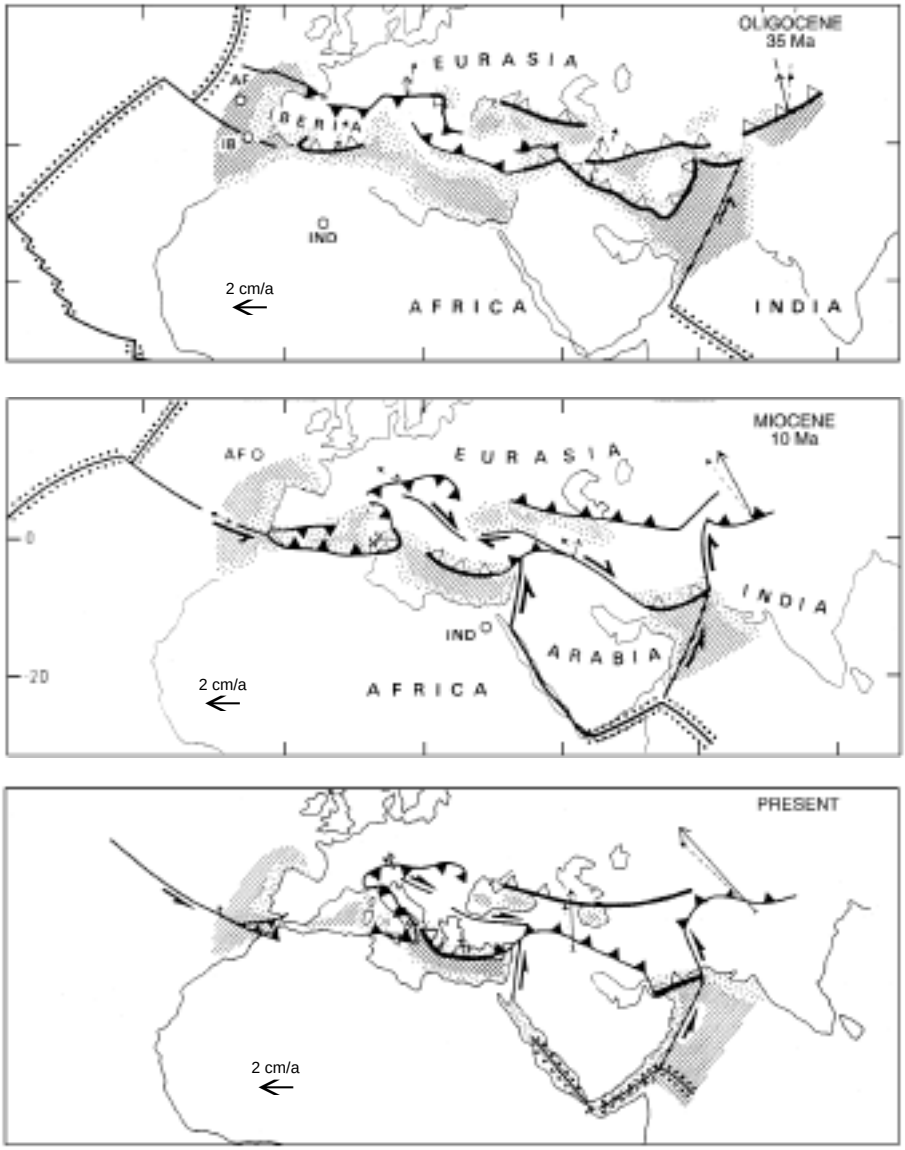

Figure 1 Paleogeographic and geodynamic reconstruction of the late Cenozoic evolution of the Mediterranean area. *Top*: situation during Oligocene times (about 35 Ma). *Middle*: late Miocene (about 10 Ma). *Bottom*: present day geodynamic sketch. Schematic plate boundaries are indicated by thick lines: arrows show transcurrent motion; open triangles represent oceanic subduction; closed triangles, continental collision; double dotted lines, oceanic accretion; thin line pattern, oceanic crust; dotted pattern, thinned continental crust. Small circles with label locate rotation vectors relative to Eurasia: AF, Africa; IB, Iberia; IND, India. Adapted with permission from Le Pichon *et al.* (1988); © Geological Society of America.

the reliability of the three dimensional wave velocity models. Assessment of uncertainty of tomographic results is often difficult, because our ignorance forces us to assume simple statistical properties for data errors, and we generally do not know how appropriate our theoretical assumptions are. In such a position, a test of how close our results are to expectations inferred from geology – often too complex or uncertain to be formally included as *a priori* information in the inversion – is a pragmatic and profitable experiment. Tomographic models are expressed as a three-dimensional wave velocity field, coarsely rendered by a discrete set of parameters, like blocks or splines. Translation into convenient quantities for geodynamics – such as temperature, lithosphere thickness, slab length – cannot be achieved by simple mathematical formulae with precisely known coefficients, and this step is also field for improvement. Comparison of expectations deriving from diverse information – such as tomography, geology, mantle dynamics, mineral physics, heat flux – is then highly beneficial for all the disciplines involved.

This paper has a slightly unusual structure. The main sectioning is geographical. After a broad overview, at a larger scale, we concentrate more specifically on a few regions where subduction is active, or has been active in geologically recent times. For each of these key areas, we first describe our own findings, and then compare them with results of a few relevant studies, often following different tomographic or seismological approaches. A brief discussion and interpretation of these different results, for each key region, then follows. A final section is devoted to a general discussion.

2 Travel time tomography

Seismic tomography maps variations of wave speed, usually calculated with respect to a background reference model, in two or, more often, three dimensions. Since the early works by Aki *et al.* (1977), at local scale, and by Dziewonski *et al.* (1977), at global scale, it has gained popularity among seismologists at a constantly increasing speed, and it is now a standard tool whose results are familiar to the entire geophysical community. Tomographic techniques have been quite extensively applied to the European and Mediterranean region in the past two decades. Continental-scale studies based on body wave travel times include, for example: Romanowicz (1980), Babuska *et al.* (1984), Granet and Trampert (1989), Spakman (1991), Spakman *et al.* (1993), Piromallo and Morelli (1997). Surface waves have been modelled, among others, by: Snieder (1988), Zielhuis and Nolet (1994a), Marquering and Snieder (1996). In the following, we will principally show images plotted from our own latest *P*-wave travel time model, PM0.5, illustrated and commented in detail elsewhere (Piromallo and Morelli, 2000b).

We have analyzed *P*-wave arrival times, at regional and teleseismic distance, from the Bulletins of the International Seismological Centre (ISC), for the period from 1964 to 1995. ISC includes body wave travel times routinely picked by contributing network operators, principally on short period permanent seismographic stations, distributed globally. The availability of stations and epicenters over our

area (Figure 2) is rather good, although quite irregular, with a concentration of stations in continental Europe, and earthquakes in the Balkan and Aegean regions. Clustering of earthquakes and stations adds redundancy of information: all seismic rays travelling from a narrow cluster of hypocenters to the same station carry the same information on deep Earth structure – providing that the spacing of rays is smaller than the scale of heterogeneity. This is the hypothesis behind the formulation of *summary rays*, now a rather standard practice in large scale tomography (*e.g.*, Morelli and Dziewonski, 1987; Gudmundsson *et al.*, 1990; Spakman, 1991; Piromallo and Morelli, 1998, 2000a). A summary ray represents a narrow bundle of individual rays, all travelling close to each other through the Earth, and describes their average properties. Summary rays greatly reduce the number of observations to deal with, and can help balance the great inhomogeneity of the geographic distribution of data. We construct summary rays by binning epicenters and stations with a grid having a resolution of 0.5° in the study region, and 5° on the rest of the globe.

Summary rays carry with them the signal of Earth structure, in terms of seismic travel times. In previous studies, we have shown that they can be effectively

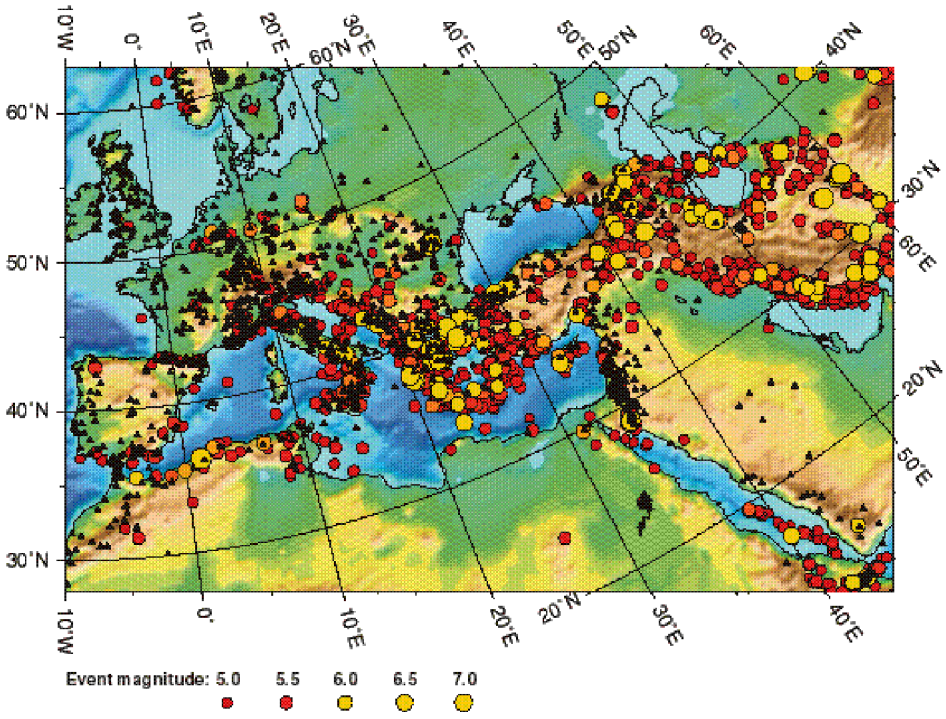

Figure 2 Distribution of permanent seismographic stations reporting to the International Seismological Centre (black triangles) and seismicity of the last 25 years (1975-1999) with magnitude greater than 4.8 (colored circles) in our study area. Oblique Mercator projection.

used, after some smoothing for continuity, to account for the heterogeneous Earth structure in earthquake location at regional (Piromallo and Morelli, 1998) and global scales (Piromallo and Morelli, 2000a). We constructed summary rays by bundling together, for each pair of cells, all rays connecting the two patches – with either source or seismograph in one of the cells. The summary travel time delay is obtained by averaging individual delays (defined as the difference between observed travel times, and those computed in a reference model, such as PREM (Dziewonski and Anderson, 1981) or sp6 (Morelli and Dziewonski, 1993).

By analysing summary delays in conjunction with the number of individual rays, it is possible to show that, in addition to random reading errors, a geographically coherent signal exists, which contributes to the variance of travel time delays by about 1.2 s^2 for regional rays, and 0.4 s^2 for teleseismic rays (Piromallo and Morelli, 1998). This is the signal we attempt to fit by updating the model of Earth structure through which we compute theoretical travel times.

In the travel time tomographic problem we need to find the three-dimensional wave velocity field $v(\mathbf{x})$ which satisfies the N observations of seismic travel times reported by all the stations for all the earthquakes available. The problem is usually tackled with a linearized perturbative formulation, assuming that we have a good initial estimate of the velocity field $v_0(\mathbf{x})$ accounting for a close estimate t_i^0 of each measured travel time t_i. We then may search for the perturbation $\delta v(\mathbf{x})$ to fit travel time delays $\delta t_i = t_i - t_i^0$. The formulation is often simplified working with the *slowness* field $c(\mathbf{x}) \equiv 1/v(\mathbf{x})$, also expressed as a background plus a perturbation field $c_0(\mathbf{x}) + \delta c(\mathbf{x})$, so that for each (summary) ray we isolate the perturbation

$$\int_{\Gamma_i} \delta c(\mathbf{x})\, dl = \delta t_i \qquad i = 1, 2, \ldots, N. \tag{1}$$

The line integral is carried out along the ray path Γ_i, calculated in the background velocity field. In nonlinear inversion schemes, the solution to system (1) is used to update the background reference model and proceed to find a new solution, iterating this process until satisfactory convergence is reached. The more common linear scheme, which we follow, instead stops the process after the first step. This is simpler and more robust when data are inaccurate (Dorren and Snieder, 1997), such as in large-scale travel time inversions where improvements of nonlinear schemes are limited to slightly sharper images where data coverage is best (Bijwaard and Spakman, 2000).

There are different approaches to solve system (1). We parametrize the slowness perturbation using three-dimensional linear splines as basis functions, thus discretizing (1) into a system of linear equations in the M spline coefficients. Existence of errors in the observations implies that we need to fit our data only within their confidence. We choose to minimize the misfit between data and model predictions in a least squares sense.

Our discretizing grid is regularly spaced by 0.5° in latitude and longitude in a rotated reference frame with the new equator in the middle of our study area, shown in Figure 2, so that cells are approximately of equal area. Our target volume includes the upper mantle and the transition zone, down to the uppermost

lower mantle to a depth of 1000 km. Depth spacing is 50 km. This brings us to a three-dimensional $121 \times 71 \times 21$ grid, and 180 411 model coefficients. Given the incomplete coverage of seismic rays, about 20% of the coefficients are not constrained by any datum and are taken out from the inversion. Solution of such large linear inverse problems cannot be based upon finding an explicit inverse matrix, but must rely on iterative techniques, suitable for tackling large underconstrained, sparse, linear systems. We use the popular LSQR algorithm (Paige and Saunders, 1982; Nolet, 1987) and a regularization condition based on minimization of the gradient of the solution.

The selection of the geometry of the target volume, and of the rays to be used, has quite material consequences on the resolution of a tomographic model. Of course, body wave arrivals from short distance, up to a few degrees – such as *Pg* or *Pn* – only provide information on the crust and the top few kilometers of the mantle. Teleseismic arrivals – with epicentral distance from 25° to 90° – cross the whole upper mantle, as these rays bottom at depths between 700 km and the core-mantle boundary. By approaching upper mantle discontinuities with steep incidence angles, they are relatively insensitive to inaccuracies of the background model (used to trace rays), and therefore provide quite robust information on lateral changes of wave velocity. Teleseismic rays were the first to be used for travel time tomography (*e.g.*, Aki *et al.*, 1977; Dziewonski *et al.*, 1977). However, each ray only provides, through (1), an integral information on the structure crossed. If all rays cross the same deck of layers, we cannot retrieve differences in wave velocity structure among these layers. For optimal sensitivity, we should use rays bottoming in the same depth range of the model. Teleseismic rays are therefore good for the lower mantle (provided they are corrected for structure above). Intermediate distance, regional body waves, bottoming in the more elaborately structured upper mantle, are very prone to being contaminated by an inappropriate reference model, but their inclusion, introduced by Spakman (1991), is very influential for improving depth resolution in the upper mantle. Consequently, we use all travel times with epicentral distance closer than 90°.

Of course, when we add paths from outside the model domain, we add rays which have also been contaminated by accruing delay travelling through heterogeneities before entering our target volume. There is the danger of mapping these unaccounted for heterogeneities – located away from the study area – into our model. The conceptually simplest solution appears to be to extend the model domain so as to cover the whole volume spanned by rays – perhaps the whole globe. The number of model unknowns increase enormously, and new problems arise from the very wide data distribution gaps, although the problem remains feasible. Some recent global whole-mantle tomographic models retain detail almost comparable to regional analyses (Grand *et al.*, 1997; van der Hilst *et al.*, 1997; Bijwaard *et al.*, 1998; Boschi and Dziewonski, 1999). However, we note that summary rays, also constructed for rays from earthquakes and stations outside the model domain, provide a convenient framework for correcting theoretical travel times for heterogeneous lower mantle structure. In fact, summary delays can be used to construct Empirical Heterogeneity Corrections (EHC) which represent the effect

of aspherical Earth structure as well as a detailed three-dimensional velocity model for earthquake location (Piromallo and Morelli, 1998, 2000a). To prevent contamination of Earth structure outside our study region, then, we can similarly employ EHC – with the caution of averaging corrections over the whole Euro-Mediterranean region so as to preserve lateral differences within the study area.

3 Images of the Mediterranean subduction belt

3.1 *The large-scale tomographic picture*

In this section we outline the major features of the structure of the upper mantle of the Mediterranean area, as revealed by seismic tomography. More detail on a few selected regions is given in the following sections of the paper. Figure 3

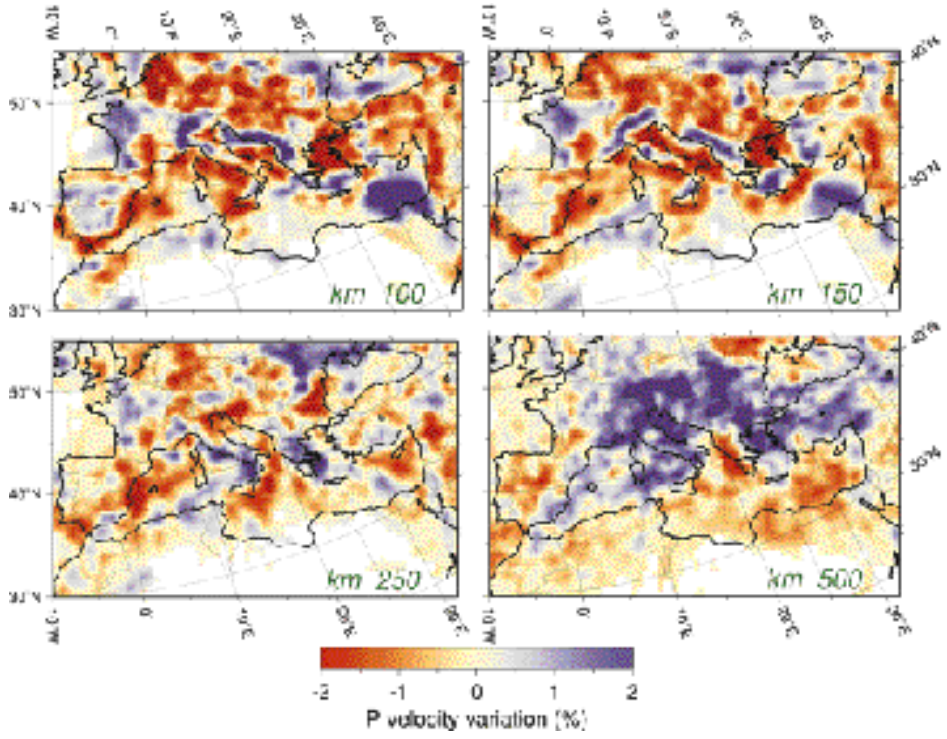

Figure 3 Maps of *P*-wave velocity variations in the central part of model PM0.5 (Piromallo and Morelli, 2000b). Velocity variations are represented by color, with scale ranging ± 2 percent with respect to average velocity at this depth. Colors turning to red mark *P* wave velocities slower than average. Shades of blue indicate relatively fast velocities. Maps are horizontal slices cut through model PM0.5 at various depths, shown in labels in the bottom right corner of each panel: 100, 150, 250, and 500 km. Oblique Mercator projection.

shows horizontal sections cut at different depths through model PM0.5. *P* wave velocity changes, with respect to the average value at each depth, are represented in different colors, with red showing slower than average regions, and blue marking faster portions. Areas not sufficiently sampled by our data set are left blank. The color scale is the same for all the panels, and covers variations of ± 2%. Qualitatively, we therefore expect subducted lithospheric material, colder and seismically faster than neighboring rock, to show up in such pictures in blue, whereas warm regions (slower) would appear red. At first glance, we can in fact identify the fast velocity trace of the Alpine orogenic belt in the upper mantle from the maps representing the model at 100 and 150 km depth (Figure 3, top panels). A well defined fast belt runs from the Northern Apennines, the Alps, Dinarides, Hellenides, and the Hellenic trench. Due to worse data coverage, North Africa is characterized by lower resolution at shallow depth, and by smaller amplitudes of the anomalies. As teleseismic rays fan out as they go deeper, their geographic coverage improves at increasing depth – as shown by the progressive retreat of the unresolved, blank, area to the south. As ray coverage improves (see maps at 150 and 250 km), a fast belt also appears under Maghrebides, joining with the fast anomaly running along the Calabrian arc. At 150 and 250 km, the Carpathians are also clearly marked by a seismically fast arc. Slow anomalies are instead present under the Tyrrhenian and the Western Mediterranean, the Aegean, and Central-Eastern Europe. Slow anomalies of the upper mantle are stronger at more shallow levels, and attenuate with greater depth (compare maps at 100, 150, and 250 km).

As we enter into the transition zone, the picture changes dramatically (Figure 3, 500 km). Now the area is dominated by a large assemblage of seismically fast material, running from Gibraltar, off the Mediterranean shore of Maghrebian North Africa, forming a wide cluster under the Alps and the Northern Adriatic, then moving East under the Balkan region and Asia Minor.

3.2 *Comparison with other models*

Results of other studies in some cases show less detail but are otherwise in general good agreement with these pictures. The existence of cold lithospheric roots below the Alps and the Northern Apennines had been recognized by earlier studies, such as by Babuska *et al.* (1984). Granet and Trampert (1989) imaged the mantle below Europe and the Mediterranean, with a rather coarse block parametrization and using teleseismic rays, and revealed a sub-vertical fast slab-like body under the Calabrian arc and the Aegean. However, the relatively small extent of their data set limited the resolution of their model.

The existence, and shape, of a cold lithospheric signal under the Alpine belt has been better imaged by Spakman (1991) and Spakman *et al.* (1993). They used a technique similar to ours, and first pointed out the improvement in depth resolution given by the joint inversion of teleseismic and regional-distance seismic rays. Spakman *et al.* (1993) also investigated the effect of two different reference

background velocity distributions on tomographic results. In fact, a strong dependence on the average, one-dimensional background velocity distributions – used as a reference for tracing seismic rays and for calculating relative variations of wave speed – is a disadvantage of using regional-distance rays. Working with two such background velocity distributions, Spakman *et al.* (1993) derived two models which differ appreciably from a quantitative point of view – mostly in terms of amplitude and depth extent of the anomalies – but generally lead to similar qualitative conclusions. Figure 4 shows sections at 95 km depth from Spakman *et al.*'s two different models, referred to two different background velocity distributions. In spite of a marked difference in the amplitude of the anomalies, we can still identify the presence of relatively faster lithosphere under the Adriatic, Dinarides and Hellenides, slow Tyrrhenian and Ligurian seas, slow Aegean, slow Balkans, Pannonian and Central-Eastern Europe, and faster Central Western Europe (barely included at the top left of the panels). These broad features agree with PM0.5 (Figure 3, 100 km) although details, sometimes important, differ, and motivate the more detailed analyses explained in the following sections.

Zielhuis and Nolet (1994a) and Marquering and Snieder (1996) modelled surface waves in the European-Mediterranean region, and found three-dimensional models for *S*-wave velocity in the upper mantle which agree with *P* travel time tomographic studies on the larger-scale features. The broader subduction zones can be recognized in *S* velocity models as fast anomalies, such as under the Hellenic region and, below 150-200 km, under the Apennines. However, the resolution offered by surface wave studies is such that the upper mantle structure cannot be resolved to as fine a detail as in *P* travel time models.

Seismic tomographic studies agree in showing a strong signature of subduction in the Euro-Mediterranean upper mantle and transition zone. Higher resolu-

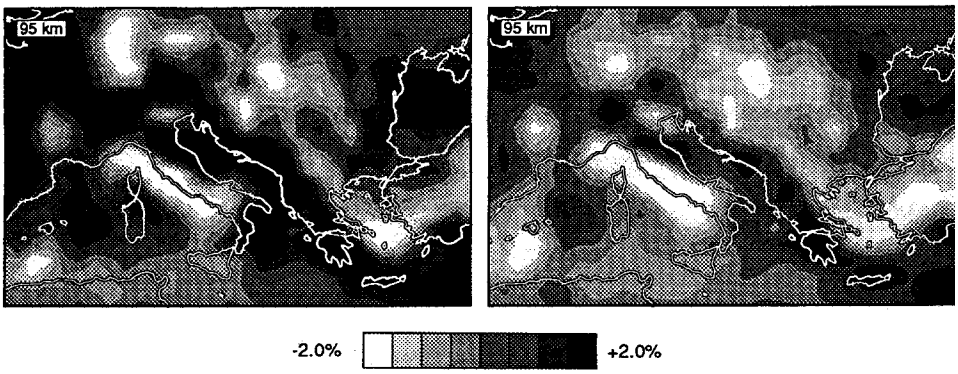

Figure 4 Comparison between models EUR89A (left panel) and EUR89B (right panel) for the Central Mediterranean area, at the depth of 95 km (from Spakman *et al.*, 1993). The two models have been computed using different background distribution of *P* velocity, used for ray tracing. Light shades of grey represent slower wave velocity. The scale is clipped at ± 2%. Reprinted with permission from Spakman *et al.* (1993); © Elsevier Science.

tion models show that the signature is rather complex, with narrow bending shapes, small-scale changes in dip and direction of the anomalies, horizontal and vertical discontinuities, and varying amplitude. These characteristics of the seismic velocity structure are important as they reflect complexity in the underlying tectonic processes. By mapping complexities in the structure of the mantle, images of the seismic velocity structure may contribute to the understanding the geodynamic evolution of the region. In the following we examine a few selected areas with more detail and add some comments on the interpretation of tomographic images.

4 The Calabrian-Apenninic arc: from subduction to delamination

4.1 *The tectonic frame*

The Tyrrhenian basin is a classic example of extensional back-arc basin, opened by the outward migration of the Calabrian arc (Malinverno and Ryan, 1986). In a subduction system, sinking of the underthrusting plate at a velocity exceeding that of plate convergence causes the line of subduction to retreat. If the overriding plate does not keep up with the retreat of the trench, a back-arc basin opens by extension. The sediment cover of the subducted plate is stripped to form an accretionary wedge, which eventually grows as an orogenic belt when the back migrating trench collides with the continental external foreland. This process caused the presence in the Mediterranean of a number of arcuate thrust belts, backed by extensional basins (Figure 5). In the Tyrrhenian extension started at about 17 Ma and progressed to the East and South-East, driven by the pull of the NW-plunging slab.

The Apenninic chain is a complex pile of thrust and nappe units, transported toward the Padan-Adriatic-Ionian-Hyblean foreland starting from late Oligocene times (Hill and Hayward, 1988), now uplifting and undergoing extension perpendicularly to the chain axis (*e.g.*, Sagnotti *et al.*, 1999). The chain is divided in two major units. The arcuate Northern Apennines border the Po plain, trending almost EW, then turn to NW-SE around Tuscany, to NNW-SSE in Central Italy. A clear and well defined feature, the NS-trending Ortona-Roccamonfina line – which acted as a dextral oblique-slip fault during Quaternary times (Patacca *et al.*, 1993) – marks the transition to the Southern Apennines. Here, the Apennines assume the dominant NW-SE direction. The Calabrian arc, further south, borders the Tyrrhenian basin to the SE (Malinverno and Ryan, 1986; Patacca *et al.*, 1993).

4.2 *The tomographic picture*

The tomographic images of the uppermost mantle of model PM0.5 show good correspondence with geologic features. The shallow mantle, at 50 km depth (Figure 6, top left panel), shows a broad region of slow *P*-wave velocity – due to temperatures higher than average – under the Tyrrhenian basin, spreading to the

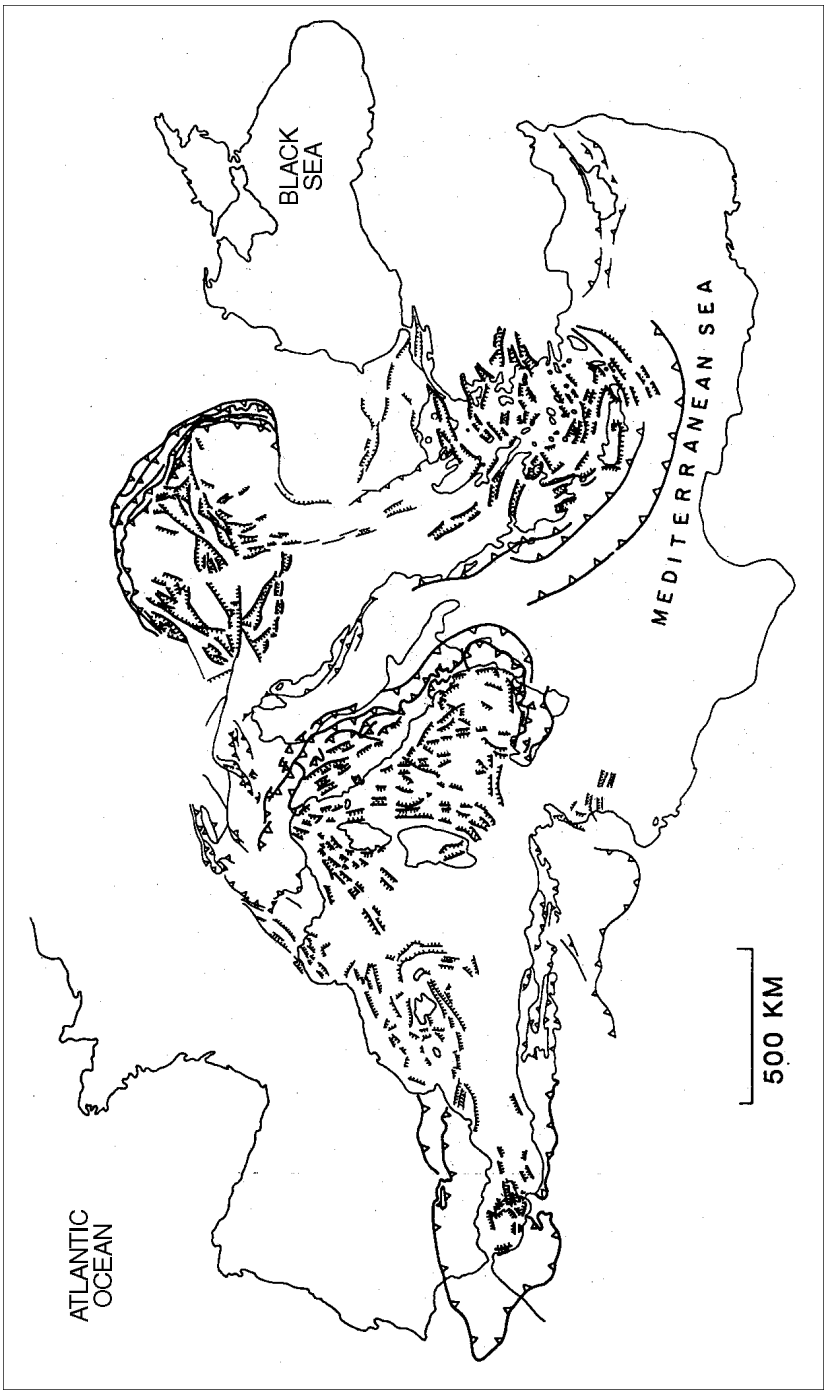

Figure 5 Late Cenozoic thrust belts and back arc basins showing contemporaneous extension. Barbed lines represent late Cenozoic thrust faults; ticked lines indicate normal faults. There are four extensional basins surrounded by coeval thrust belts; from east to west: the Aegean-Hellenic system; the Pannonian-Carpathians system; the Tyrrhenian-Apennines system; and the Alboran-Rif-Betic system. Reproduced with permission after Royden and Burchfiel (1989); © American Geophysical Union.

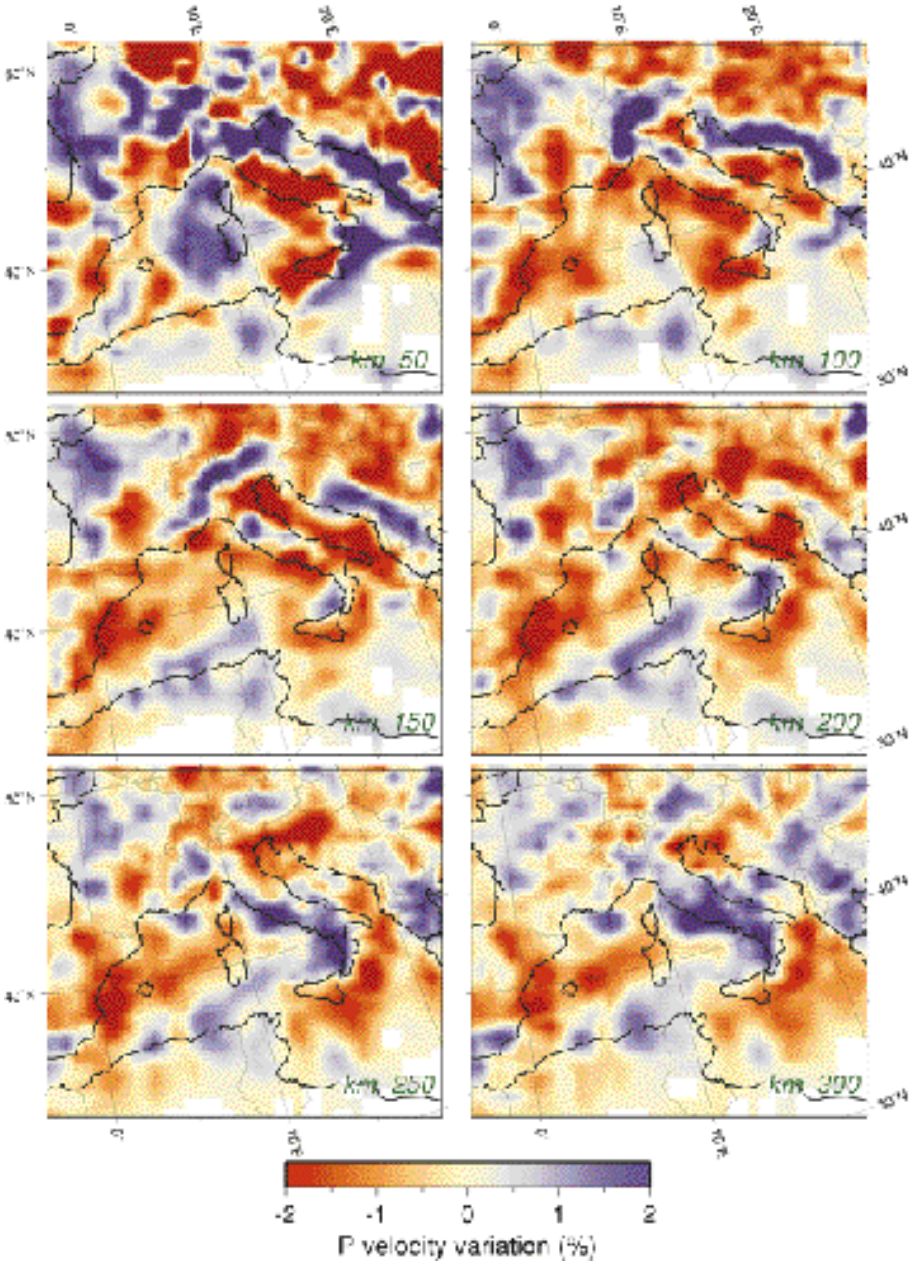

Figure 6 Maps of *P*-wave velocity variations in the Tyrrhenian region in model PM0.5. Velocity variations are represented by color, with scale ranging ± 2 percent with respect to average model. Red is slow, blue is fast. Maps are horizontal slices at various depths in the model: 50 km, 100 km, 150 km, 200 km, 250 km, and 300 km.

Sicily channel, to the southwest, and to the Apennines. Fast velocity is instead present under Calabria. The Corsica-Sardinia and Balearic lithospheric blocks are also characterized by fast velocities, also present under the Adriatic region and under the Po plain. A narrow, well defined, fast ribbon underlies the Dinarides and Hellenides. Velocity anomalies at this depth are mainly controlled by *Pn* rays and reach values of ± 4% with respect to the regional average.

At 100 km depth (Figure 6, top right) the picture is quite different. The slow Tyrrhenian anomaly is less intense, but still present, stretching farther to the West under Corsica and Sardinia, and under the Ligurian Sea. The Northern Apennines now show as a narrow, fast anomaly, continuing to the northwest, and becoming stronger under the Alps. This fast strip then runs along the Dinarides and Hellenides, without interruption. An apparently isolated fast mass is also present under Calabria. The Southern section of the Apennines is distinctly different from the northern section, and has slow *P*-wave velocity at this depth.

Going deeper, at 150 km (Figure 6, center left), the difference between Northern and Southern Apennines is maintained. Here, the signal of cold subducted lithospheric material is particularly clear. We can follow a fast-velocity strip – in blue – winding around with an *S* shape, with bends corresponding to the Calabrian and Alpine arcs. This fast strip is bordered by a slower-than-average *P*-wave velocity background – in red. The fast belt runs almost continuously from North Africa, under Calabria, Northern Apennines, Alps, Dinarides, Hellenides. The fast belt is interrupted under the Sicily channel, Southern Apennines, and at the junction between Alps and Dinarides.

Anomalies become weaker at 200 km depth (Figure 6, center right). Here, the fast belt gains continuity between the Northern African and the Calabrian anomalies. As depth increases, this fast region is clearly shifting from under Calabria to the NW, under the Tyrrhenian. The Southern Apennines gap decreases in size. The fast anomaly under the Alps weakens in the western section, and disappears in its eastern reaches. The slow signal under the Tyrrhenian has almost disappeared.

As we go even deeper, at 250 km (Figure 6, bottom left), the pattern of high velocity anomalies which bounds the Tyrrhenian gains amplitude and continuity. The Northern and Southern Apennines are here joined in a single continuous, wider, belt, backed by slow material in the Ionian Sea. Also note the position of fast material under the South Tyrrhenian shifting to the NW as depth increases, to shape a NW-dipping slab, which shows very well in a vertical cross-section to appear below. The fast anomaly under the Dinarides disappears already at 200 km depth, but the Hellenides remain fast.

At 300 km (Figure 6, bottom right), finally, a wide, irregular, lump of fast velocity is concentrated near the center of the figure, still connected to North Africa. It can still be followed under the Alps, and under the Hellenides. Slow anomalies are at this depth much less intense than in shallower maps.

Two vertical cross-sections in the three-dimensional model are shown in Figure 7. Cross-section A-a is drawn across the Tyrrhenian fast anomaly and shows that a well-defined, continuous, fast-velocity slab dips approximately 45° to the NW and bends to assume a nearly horizontal posture in the transition zone. Fast

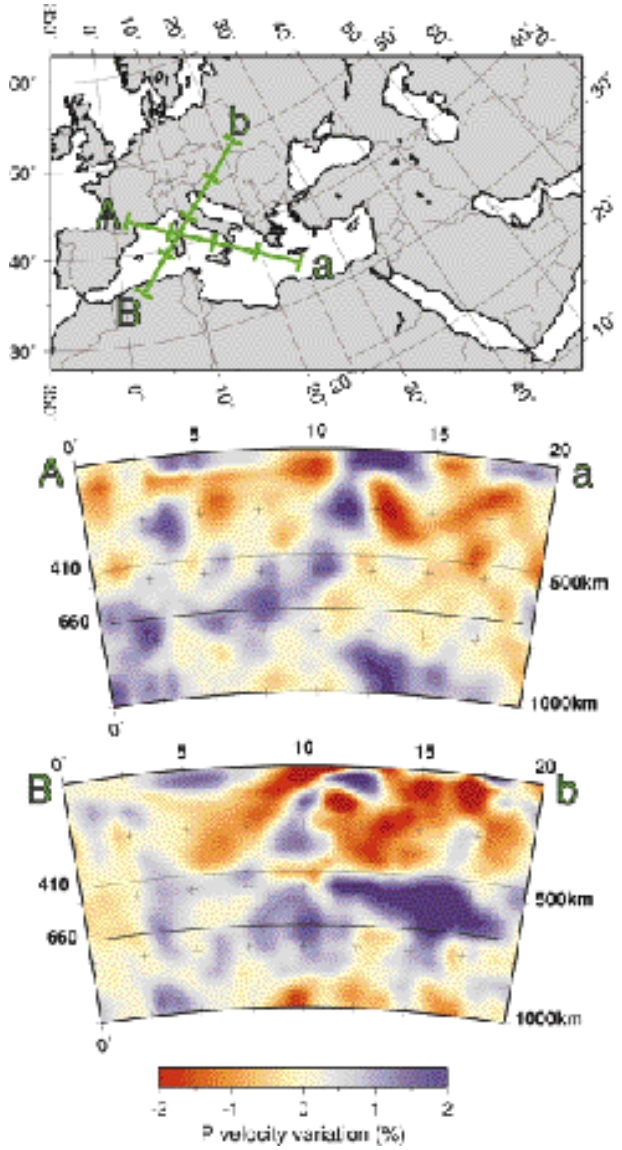

Figure 7 Vertical cross-sections across the Tyrrhenian Sea and across the Northern Apennines in model PM0.5. Relative velocity variation with respect to vertically-varying background model is represented by the same color scale of Figure 6. The surface traces of the two cross-sections A-a and B-b are shown in the map on top and are great circle arcs. Horizontal distance from the origin of each cross section, in geocentric degrees, is indicated on top of the section (0°, 5°, 10°, 15°, and 20° correspond to ticks in the traces plotted on the map). Transition zone discontinuities (at 410 and 660 km depth) are marked by a thin continuous line. Crosses are spaced 250 km in depth, and 2.5° laterally.

material reaches the lower mantle. The Tyrrhenian is marked by a shallow low velocity anomaly, especially in its SE margin (approximately at 10° distance along the section), which is overlain by the fast Corsica-Sardinia block. Cross-section B-b in Figure 7 cuts instead across the Northern Apennines. Here, a SW-dipping fast anomaly is shown, overlain by the shallow slow anomaly on the Tyrrhenian side, that we already saw in the map at 50 km. The fast material apparently runs all the way down to the broad assemblage located in the transition zone.

4.3 *Comparison with other models*

Features similar to those seen in PM0.5 are also present in other models in the literature. Our previous calculations, limited to a smaller model domain and fewer data (Piromallo and Morelli, 1997), showed similar results. Similar belts of fast velocity are also shown by model EUR89B (Spakman *et al.*, 1993) to run under the Northern Apennines, the Alps, the Dinarides and the Hellenides. EUR89B also agrees in imaging the shallowest mantle (about 50 km depth) slow under the Apennines and the Tyrrhenian coast of Central Italy, but the slow anomaly grows wider and stronger approaching 100 km depth, in contrast with the opposite trend exhibited by PM0.5. EUR89B has reduced resolution at this depth in the Tyrrhenian, Sicily and further south, perhaps due to fewer paths connecting North Africa to Italy in their database – ISC Bulletins until year 1982. Inclusion of data from later years proved to be highly beneficial to improve the imaging capability in areas close to North Africa – likely because of recent improvements in seismographic coverage in the area. As a result, the signal of cold African subducted lithosphere, absent in EUR89B, is instead clear and unambiguous in model PM0.5, especially at 200 to 300 km depth. The difference in ray coverage may also account for generally lower amplitude of anomalies in the Southern Tyrrhenian of model EUR89B.

Mele *et al.* (1996, 1997) estimated the *P* and *S* attenuation structure of the uppermost mantle beneath the Italian peninsula and neighboring seas. They used a spectral ratio technique to analyze *Pn*, *Lg* and *Sn* phases on digital waveforms recorded by short period seismographs of the Italian national network for earthquakes at distances between 250 and 1600 km. They found very efficient wave propagation through Adriatic lithosphere and under the Po plain, and, in contrast, inefficient propagation in the uppermost mantle beneath the Apennines, the western margin of the Italian peninsula, and the Tyrrhenian basin. This is in very good agreement with our findings, if we assume that high velocity correlates with high *Q* in a relatively cold and rigid lithosphere, such as under the Adriatic and the Po plain, and that both low velocity and high attenuation characterize warm asthenospheric material.

Pn regional arrivals have also been used to tomographically image variations in both seismic velocity and azimuthal anisotropy in this area (Mele *et al.*, 1998; Hearn, 1999). Existence of azimuthal anisotropy in the upper mantle is commonly recognized as being due to alignment of olivine crystals, or to planar intrusion of

dykes. *Pn* travel times are expected to be very sensitive to it. To include anisotropy coefficients in a tomographic inversion adds degrees of freedom and, hence, further ambiguity. This is particularly true in a region where most of the sampling derives from sub-parallel rays running from earthquakes in the Hellenic and Aegean, from the SE, to seismographic stations in Europe, to the NW. Travel times can be satisfied (almost) equally well by volumetric velocity perturbations, or by anisotropy, alone. On the other hand, if anisotropy is indeed important, the same unbalance in data coverage can bias a model neglecting anisotropy. Hearn (1999) showed with tests that appropriate choice of damping coefficients can lead to valid results. Anisotropic tomographic *Pn* models of Italy and surrounding areas (Mele *et al.*, 1998; Hearn, 1999) show the same main features evidenced by PM0.5: a 4-5% faster-than-average anomaly following the Ionian, Adriatic, and Po plain, and a similarly strong, slow, anomaly underlying the Tyrrhenian, the Apennines, and the Western Alps. Including anisotropy in the inversion allowed Hearn (1999) to obtain images which better follow surface tectonic lineaments, and better correlate with PM0.5 – an isotropic model. Even though anisotropy can therefore bias studies based on *Pn* rays alone, its effect on models deriving from inversion of data sets with rays having different geometries – local, regional, teleseismic distance – and criss-crossing with different incidence angles, appears to be unimportant. It adds to the unmodelled signal – commonly assumed to be noise – but it does not bias results.

Lucente *et al.* (1999) used teleseismic ray *P* and *PKP* delay times, individually picked from recordings of the Italian short period national network, for a tomographic inversion, covering Italy and surrounding seas, from the crust to 800 km depth. They used a very classic and well tested tomographic technique, known as ACH from the names of the authors who introduced it (Aki *et al.*, 1977). Their main finding is an intermittent, but almost continuous, high velocity body (up to 3-4% faster than average) located under the entire length of the Apennines, between 250 and 600 km, dipping toward the Tyrrhenian area. This anomaly continues upward, between the crust and 250 km, mainly under the Northern Apennines and Calabria. This picture agrees qualitatively with our images, where a fast anomaly is also present at these depths and regions. Lucente *et al.* (1999) fail instead to image the slow *P* wave velocities in the shallowest mantle under the Apennines, present in PM0.5 and in the other studies referenced above. This can likely be ascribed to deficiency of depth resolution typical of the ACH scheme, which only uses steep incidence angle rays crossing the whole thickness of the model (Lévêque and Masson, 1999).

4.4 *Interpretation and discussion*

All tomographic models discussed above reveal the presence of fast material at depth under the Apenninic arc – unanimously interpreted as the signature of subducted lithosphere – and a shallow slow Tyrrhenian anomaly. This global picture is in agreement with expectations based on the mechanism of the opening of

the Tyrrhenian basin in the convergent Africa-Eurasia regional setting, involving rollback of the subduction front. Rollback induced stretching and extension of the Tyrrhenian crust, causing hot asthenospheric material to rise. Back arc migration caused progressive increase of arc curvature, and counter-clockwise rotation of the strike of subduction under the Apennines.

The vertical continuity of the slab under the whole Apenninic belt is instead a point of variance among the different models. It is a significant point as it has consequences for the timing and the character of termination of subduction. The Apennines are uplifting and extending, showing that the geodynamic picture has changed since their origin as a thrust and nappe belt piled up scraping the sedimentary cover of the lower plate in a subduction environment. Subduction is evidenced by the fast (and cold) lithospheric material, consistently revealed by all tomographic studies to date. Active subduction is documented under the Calabrian arc by intermediate depth seismicity outlining a Benioff zone dipping to the NW under the Tyrrhenian. To reconcile evidence of active subduction with quaternary uplift of Southern Italy, Westaway (1993) hypothesized that the slab is broken, and still sinking by its negative buoyancy while the lithosphere is readjusting isostatically, rebounding up as a response to removal of the downward slab pull (Davies and von Blankenburg, 1995).

A slab discontinuity is not really seen in any tomographic model in the Calabrian section, but some models (Spakman *et al.*, 1993) show no apparent connection between the Adriatic plate and the subducted lithosphere elsewhere under the Italian peninsula. This lead Wortel and Spakman (1992) to propose a model of lateral progression of the tear in the subducted slab, initiating in the NW and gradually migrating to the SE (van der Meulen *et al.*, 1998).

The evidence for a NW-to-SE progressive slab detachment, proposed by the Utrecht University group, is not shared by all models. Teleseismic tomographic models (*e.g.*, Amato *et al.*, 1993; Lucente *et al.*, 1999) do not reveal slab detachment, but rather image a seismically fast body perhaps more continuous vertically than horizontally. The limited vertical resolution of teleseismic rays – all crossing the upper mantle with similar and very vertical incidence angle – might explain that a shallow slow anomaly is in fact obscured by a strong, deeper, one. However, signs of vertical continuity of the Adriatic slab can also be followed in our most recent model – although with lateral variations along strike.

Analysis of PM0.5 (Figures 6 and 7) shows that distinct situations exist under Calabria, the Northern and the Southern Apennines. The Calabrian slab is identified by a continuous trace of high velocity, from the shallow lithosphere to the transition zone and below (Figure 7, cross-section A-a). The seismically fast material – colder and denser than ambient rock – appears to be deflected by the 670 km discontinuity, to pool in the transition zone before sinking into the lower mantle.

Under the Northern Apennines we can also follow higher than average velocity from 100 km depth, to the transition zone. A low velocity anomaly is confined to the very top of the mantle (see Figure 6, 50 km). The general situation is well depicted by cross-section B-b in Figure 7. Difference with respect to Calabria is clear: the slab is thinner, and overlain by a slow anomaly.

Under the Southern Apennines the fast belt only appears below 200 km, and then remains strong, at greater depths, to merge into the broad aggregate of the transition zone. Above 200 km depth, a wide discontinuity in the subducted slab clearly appears instead under Southern Italy. The boundary between the different behaviors of the lithosphere of the Northern and the Southern Apennines runs in correspondence with a well known surface geologic lineament, the Ortona-Roccamonfina line. Differences in upper mantle structure therefore support the view that the Northern and Southern Apennines are two rather different provinces, which followed different evolutionary histories (*e.g.*, Patacca *et al.*, 1993). It is possible that subduction continued longer, although in a different way, under the Northern Apennines, where presence of hot asthenospheric material at shallow depth, above a dipping lithospheric layer (see Figure 7), agrees with geochemical and petrological data (Serri *et al.*, 1993) to delineate a picture compatible with a model of continental lithospheric delamination (Reutter *et al.*, 1980; Nelson, 1992). Subduction is instead still active under Calabria, where the slab appears to be connected with the Ionian lithosphere (Figure 7) but shows a limited lateral extent above the depth of 200 km (see maps in Figure 6). Lateral tears, from both sides of the slab, presumably developed in the last 2 Ma, triggering volcanism and influencing the neotectonic evolution of the region (Argnani, 2000).

5 The Betic-Rif arc: subduction or delamination?

5.1 *The tectonic frame*

The Betic (Southern Iberia) and Rif (North Africa) mountain belts are the westernmost thrust belts of the Alpine system (Horvath and Berckhemer, 1982). They form an arc (Gibraltar arc) surrounding the extensional Alboran basin to the N, W, and S (Figure 5). Thrusting along the belt, and extension in the basin, are coeval, having occurred from Miocene (say, 20 Ma) to present, when Africa and Eurasia continuously converged. Several tectonic models have been proposed to explain extension, and contemporaneous outward thrusting along the margins of the basin: competing models call either for the existence of a rigid Alboran microplate (*e.g.*, Udias *et al.*, 1976), subduction rollback (*e.g.*, Lonergan and White, 1997), or lithospheric delamination (*e.g.*, Seber *at al.*, 1996a) to account for the observations.

Shallow seismicity is rather diffuse in this area, being present in the Betic and Rif crust and under the Alboran Sea. Intermediate depth seismicity extends down to 150 km. Below this depth, only three deep, isolated, earthquakes are known to have occurred beneath Granada in 1954, 1973, and 1990 (Chung and Kanamori, 1976; Grimison and Chen, 1986; Buforn *at al.*, 1988, 1991), possibly revealing the presence of cold lithosphere at a depth of 600 km. The discontinuous depth distribution of seismicity has been interpreted as consistent with convective removal of

lithospheric mantle (Seber *at al.*, 1996a) or, alternatively, with subduction, terminated 12-15 Ma ago, leaving a detached block of slab (Lonergan and White, 1997). A subduction model must explain that the paleogeographic reconstructions of relative Africa-Eurasia motion (Figure 1) do not indicate sufficient amount of shortening to subduct material down to 600 km depth (Le Pichon *et al.*, 1988). This is accomplished by postulating – consistently with other evidence – a rather long retreat of a curved subduction front, from the east to the west (Lonergan and White, 1997), which would have contributed enough sinking lithosphere without requiring much NS convergence.

5.2 *The tomographic picture*

The layer at the top of the mantle in model PM0.5 (50 km, Figure 8, top left) shows a wide slow-velocity area beneath the Alboran Sea and the Strait of Gibraltar, surrounded by a ring of fast velocity roughly following the thrust faults (compare with Figure 5). The slow anomaly continues along the Mediterranean Iberian coast, and the North African coast, covering the area of distribution of Neogene volcanism (*e.g.*, Lonergan and White, 1997).

Deeper, at 100 km (Figure 8, top right) the slow Alboran velocity anomaly becomes slightly stronger, exceeding –2%, and it widens to cover the Valencia Trough, as well as most of the Algero-Provençal basin. The fast ring is not very evident, also because of limited data density: faster-than-average velocities are mostly confined under the Moroccan Pre-Rif. A (weak) fast linear feature is visible under Algeria and Tunisia. Its amplitude may be attenuated by the limited amount of data available.

At 200 km, anomalies are rather weak in the Alboran region (Figure 8, center left). At this depth, a continuous – although weak – fast velocity body striking NE-SW extends across the Alboran Sea, from Iberia to Africa. The North African fast-velocity linear feature, much clearer and stronger at this depth, is shifted to the north, and here it runs continuously from the Algerian coast to the South Tyrrhenian, reaching amplitudes of 1.5-2%. A strong slow anomaly continues to be present under the Valencia Trough. A weaker, wide, slow anomaly is centered under the Gulf of Cádiz.

At the depth of 250 km (Figure 8, center right), the same features appear more clearly. The fast Alboran sheet is stronger, and a narrow, continuous, fast belt runs from the Algerian coast to the South Tyrrhenian Sea, and around the Tyrrhenian Sea along the Italian coast. The strong slow anomaly under the Valencia trough is still present.

The fast sheet cutting through the Alboran region is even stronger at greater depth (350 and 450 km, see Figures 8, bottom panels) where it reaches amplitude beyond +2%, and where it assumes a curved shape, but it is mostly confined to Alboran and Southern Iberia. Elsewhere, the amplitude of anomalies decreases. As we enter into the transition zone (Figure 8, 450 km) fast material gathers under the Western Mediterranean basin.

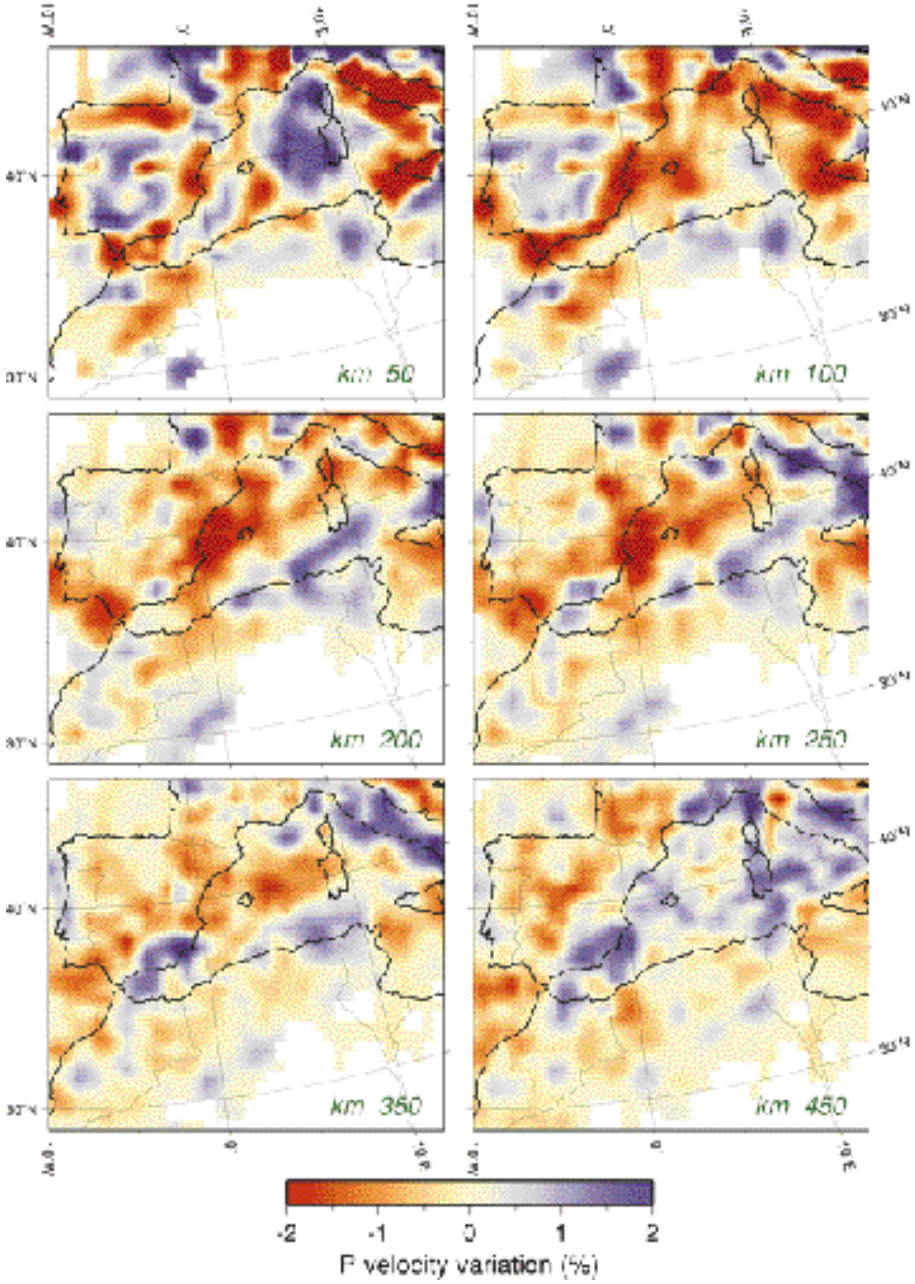

Figure 8 Maps of *P*-wave velocity variations in the Western Mediterranean according to tomographic model PM0.5. Color-coded velocity representation as in Figure 3. Maps are horizontal slices cut at depths of 50, 100, 250, 300, 350, and 450 km.

Figures 9 and 10 show 4 vertical cross-sections which help to understand the three-dimensional spatial extent of the anomalies. Sections A-a and B-b in Figure 9 are cut with slightly different strikes, along the SE-NW trending fast sheet visible on the maps deeper than 200 km. Section B-b, plotted along the strike of the fast sheet, shows that the fast material is principally confined between the depths of 250 and 410 km, but it appears to be connected to shallow fast structures with continuity, and to penetrate to greater depths. The Alboran basin is underlain by a slow uppermost mantle anomaly, positioned just above the main lump of fast material. Cross-section A-a, with a more NE orientation, shows that the fast anomaly, positioned deep below Alboran and Southeastern Iberia, extends under the Rif,

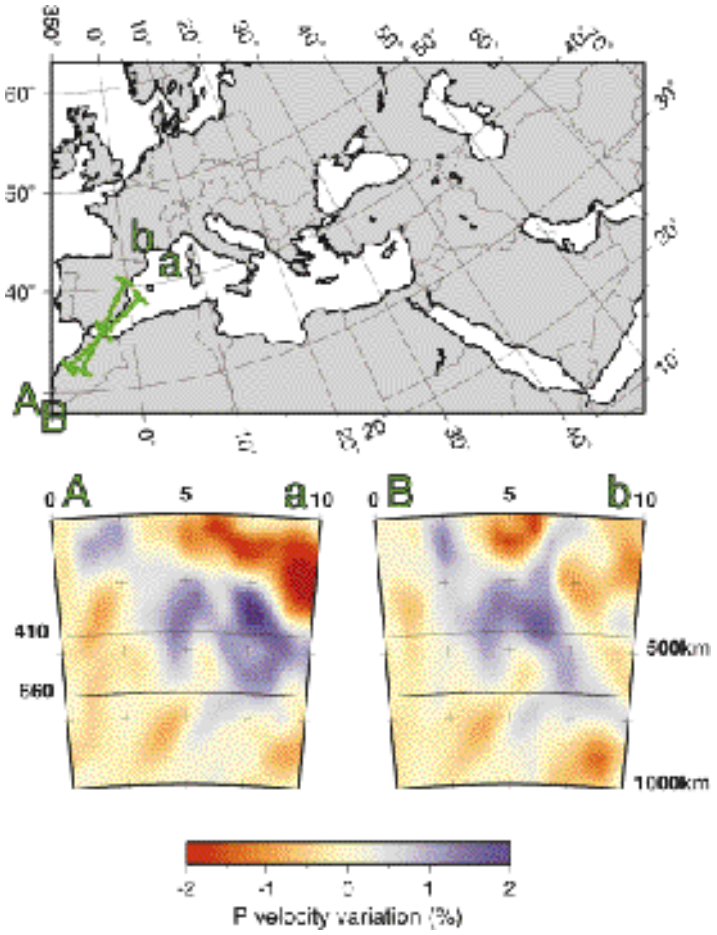

Figure 9 Vertical cross-sections in model PM0.5, revealing seismic structure below the Alboran Sea and surrounding regions. Color-coded velocity representation as in Figure 3, cross section conventions as in Figure 7. Each cross-section is 10° long at the surface.

with shallowing depth. The slow Alboran Sea anomaly evidently continues to the East with stronger and deeper characters.

Sections A-a and B-b in Figure 10 are approximately perpendicular to the previous ones, and show the intermittent vertical continuity of the fast sheet located under Iberia. Cross-section B-b shows continuity between the shallow fast velocity Iberian lithosphere, and the upper mantle and transition zone high velocity lump under Alboran.

The connection is however rather feeble, and it is interrupted more to the west, where – with this strike – the fast sheet assumes an isolated and vertically elongated shape (see cross section A-a).

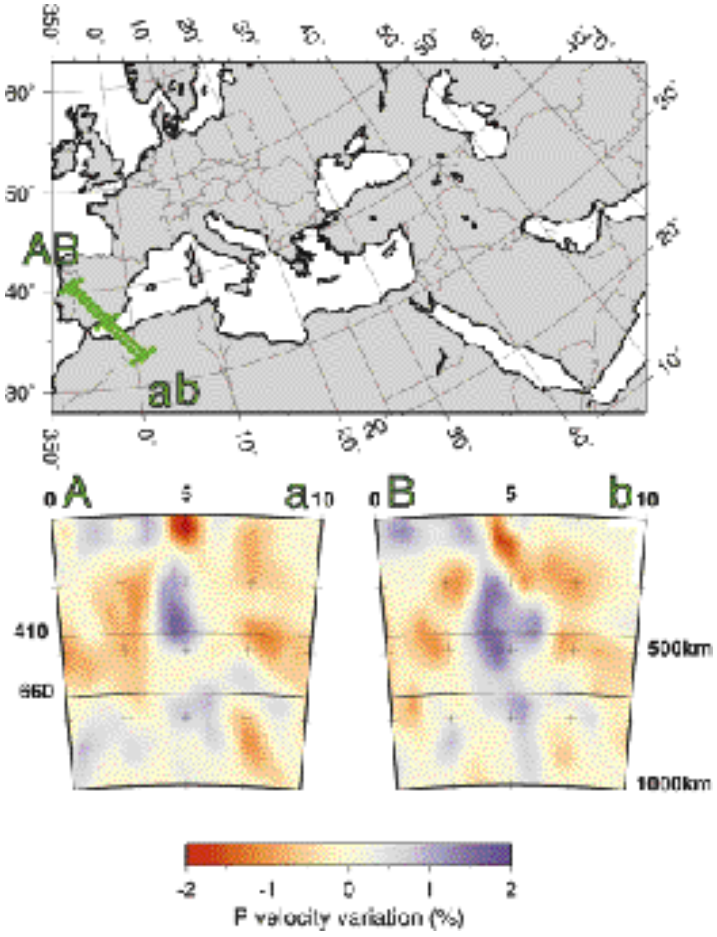

Figure 10 Vertical cross-sections in model PM0.5, revealing seismic structure below the Alboran Sea and surrounding regions. Same conventions as in Figure 9.

5.3 *Comparison with other models*

A large positive velocity anomaly, located below Southern Spain, at depths between 150 and 700 km, has also been imaged by the large scale travel time inversion by Spakman *et al.* (1993), and, with better detail, by Blanco and Spakman (1993), who also elaborated on the significance and reliability of this feature, and on its interpretation as a subducted lithospheric slab, possibly detached from the surface. The latter study, in particular – focussed on the Iberian peninsula, Alboran Sea and the Rif-Betic region – imaged the fast Southern Iberian feature showing similar characteristics as model PM0.5. Seismically fast material is concentrated in a body, elongated along a SW-NE direction, almost vertically dipping if seen across its strike. Maximum relative velocity variation reaches +2%. Blanco and Spakman (1993) fail instead to reveal significant anomalies in Northern Africa. We infer that the improvement of imaging power of PM0.5 in North Africa is primarily due to the availability, through the ISC, of high quality data from the recently installed digital seismographic network in Morocco (Seber *et al.*, 1996b).

Seber *et al.* (1996a) used teleseismic travel time residuals, recorded by seismic networks in Morocco, in a tomographic inversion to produce a three-dimensional velocity image of the upper mantle. Their result indicate the existence of a high-velocity (~ 3%) body in the upper mantle beneath the Eastern Rif and Alboran Sea, extending down to the bottom of their model (350 km). This high-velocity layer, interpreted to be delaminated rigid lithosphere, is overlain by a very low velocity uppermost mantle material, imaged by *Pn* waves, interpreted to be asthenospheric material replacing the delaminated lithosphere. In a larger scale study, Calvert *at al.* (2000) also image a high velocity body striking NE-SW from lithospheric depth to about 350 km. Between 350 and 500 km anomalies lose amplitude, but reappear in the deeper portions of the model (650 km). The authors acknowledge that the interruption of the fast anomaly in the 350 to 500 km depth range is possibly not a robust feature of the model. Mainly on the basis of geological evidence, however, Calvert *at al.* (2000) discard the possibility of a continuous subducted slab.

5.4 *Interpretation and discussion*

Seismic tomographic studies agree in revealing the main characters of the structure beneath the Alboran Sea: seismically slow material, at shallow depth, underlain by a fast body. However, details of these models differ, as do geodynamical interpretations: Blanco and Spakman (1993) interpreted the origin of the fast material as due to subduction; whereas Seber *et al.* (1996a) and Calvert *et al.* (2000) concluded that it has been brought to depth by lithospheric thickening and subsequent delamination (see also Houseman, 1996). In fact, the shallower mantle structure appears to be consistent with a delamination model: a seismically fast body underlies slow uppermost mantle beneath the Alboran Basin – a pattern likely due to sinking of cold lithospheric mantle, replaced by hot asthenospheric

material. However, the deep seismic activity of Southern Spain, and the deep fast velocity anomalies consistently imaged by tomographic studies, cannot be easily explained by a shallow mantle process. A fast velocity anomaly is actually imaged throughout the upper mantle, with local vertical continuity. In consideration also of a number of geologic observations – such as eastward continuity of Alboran crustal characters to the whole Western Mediterranean basin, and vertical-axis rotations evidenced by paleomagnetism (Lonergan and White, 1997) – it appears difficult to rule out retreating subduction as the principal mechanism responsible for the extensional regime of the basin (Figure 11). The scarcity of deep seismic activity may show, however, that subduction is no longer active. The complex

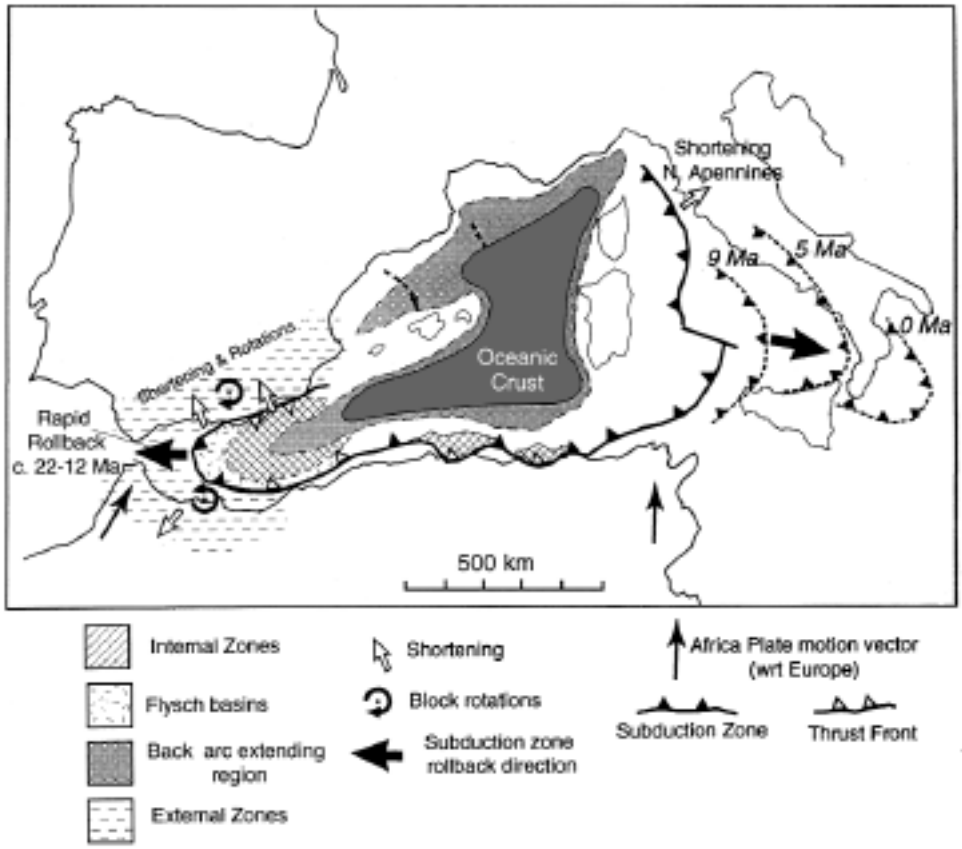

Figure 11 Reconstruction of Neogene evolution of the Western Mediterranean. The subduction zone, previously located more to the north, and straight, rolled back to hit the North African platform. Retreat continued laterally, giving origin to two arcs and opening the Tyrrhenian and Alboran Seas. Adapted with permission from Lonergan and White (1997); © American Geophysical Union.

shape and extension of the fast anomaly contributes to delineate a picture where subduction has perhaps come to an end, and some process of lithospheric removal under the basin has allowed hot asthenospheric mantle to rise to uppermost mantle depth. Details of this picture will become more clear as our knowledge of the mantle structure improves.

6 Terminal subduction: the Carpathians arc

6.1 *The tectonic frame*

The thrust belt system which runs from the Western Alps to the Eastern Carpathians (Figure 12) represents the northernmost part of the wide Alpine-Mediterranean compressional belt (Horvath and Berckhemer, 1982). The Alps and the Carpathians share many common characters (Royden and Burchfiel, 1989). Both form mountain arcs, convex toward the undeformed Eurasian foreland. Their development began in the Mesozoic, with the continental extension process which formed a narrow oceanic zone and which was then followed, since Cretaceous times, by closure of the ocean and continental collision. The convergence between the subducting European foreland, and Apulian continental fragments originated the Alps and the Carpathians.

In spite of these similarities, however, very different styles stand out, as a result of differing conditions during the recent development. The Carpathians surround an extensional back-arc basin, the Pannonian basin, created by slab roll-

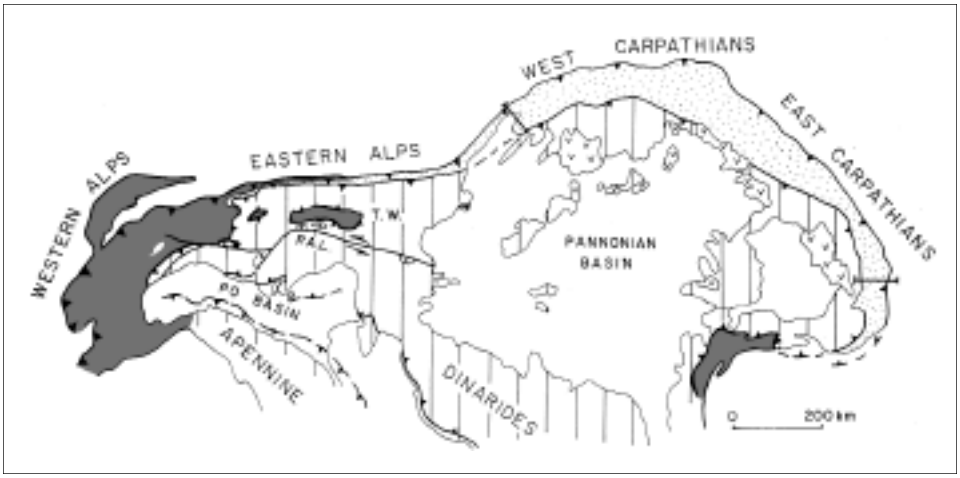

Figure 12 Tectonic map of the Alpine-Carpathians belt. Shaded area represents parts of the Eurasian plate involved in the Alpine deformation. Vertical lines represent region of combined Apulian-East Carpathian/Rhodopian fragment. Dots represent area of flysch nappes. Adapted with permission from Royden and Burchfiel (1989); © American Geophysical Union.

back since the Miocene and until recent times. In contrast, no internal extensional basin is present in the Western Alps. Here, the rate of overall plate convergence, driven by the motion of the major plates, has been larger than the rate of subduction. Other important differences are that the Alps are characterized by high topographic elevation, and large amount of erosion. High-grade metamorphic rocks are exposed, and the crystalline basement is involved in the thrusting. These features are absent in the Carpathians, a thrust belt with little or no involvement of the crystalline basement, only low-grade or no metamorphism, low elevations, and little erosion. Royden and Burchfiel (1989) pointed out the differences in development style of the two belts and the diversity of their boundary conditions during formation: the Western Alps developed as a result of convergence between the large Apulian and Eurasian plates, whereas the formation of the Carpathians has

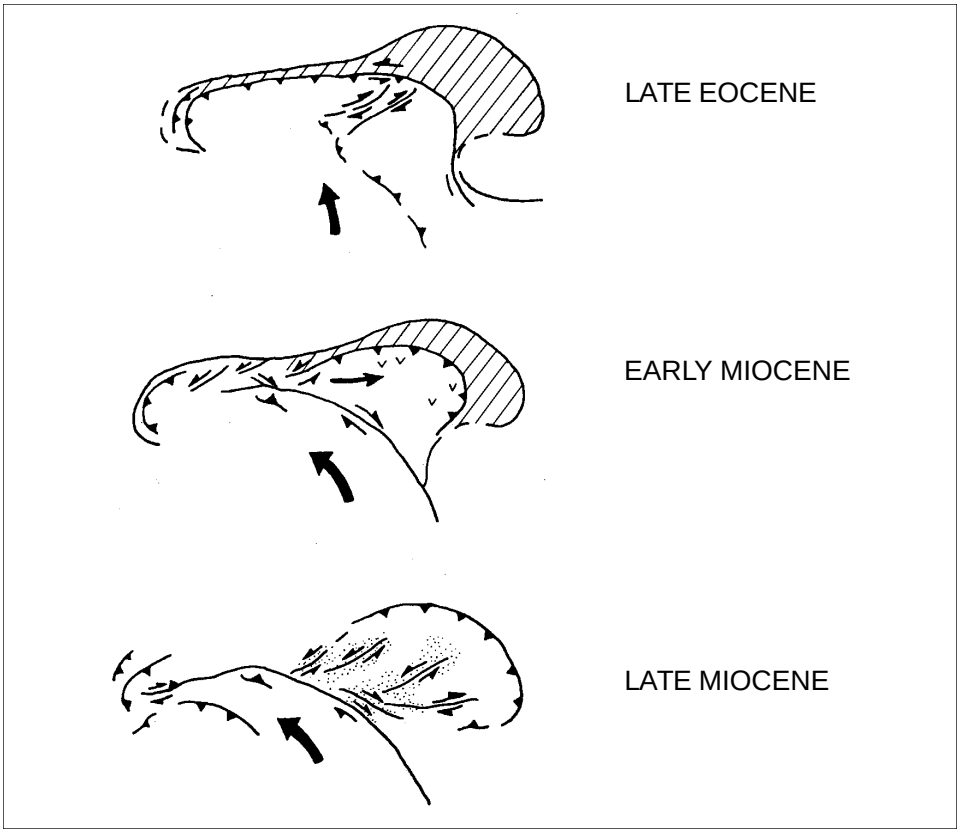

Figure 13 Schematic diagram of Tertiary evolution of the Alpine-Carpathians belt, showing motion (thick arrow) of the combined Apulian-East Carpathian/Rhodopian fragment with respect to Eurasia. Diagonal lines represent Carpathian and Rhenodanubian flysch basins. Small dots are regions of extension in the Pannonian basin. Adapted with permission from Royden and Burchfiel (1989); © American Geophysical Union.

been driven by local motion of small lithospheric fragments, which could not follow the velocity at which oceanic crust was consumed. The overall rate of convergence was thus less than the overall rate of subduction, generating retreat of the trench.

The Cretaceous convergence event affected the two belts in a similar way, subducting oceanic crust beneath the Apulian plate eastwards, southwards, and westwards (Royden and Burchfiel, 1989). Tertiary evolution initially involved subduction of continental crust – first in the Western Alps, progressively later in the Eastern Carpathians. While continental collision occurred in the Western and Eastern Alps, convergent motion between Apulian and Eurasian plates was mostly taken up, in the East, by shortening of continental crust in the Dinarides, rather than in the Carpathians (Figure 13). Since the Miocene, then, kinematics in the Carpathians was not directly controlled by the Apulian-Eurasian convergence, but rather by the relative motion of the smaller Pannonian fragment and the Eurasian plate. As an effect of the overall plate convergence here being smaller than the rate of subduction, rollback of the slab occurred between 16 Ma and 2 Ma over a distance of 600 km, followed by slab break-off when retreating subduction was stopped by the narrow passage between the East European continent and the Moesian plate (Linzer, 1996).

In the Carpathians and Pannonian region, shallow seismicity is widespread and rather diffused. Intermediate-depth seismicity – with focal depth between 70 and 200 km – is instead concentrated in a small, almost vertical, volume (about 30×70 km) below the easternmost elbow of the Carpathians range, the Vrancea region (Lorenz *et al.*, 1997; Fan *et al.*, 1998; Wenzel *et al.*, 1998). This is a rather active spot: averaged seismic moment release rate has been estimated at 7.5×10^{20} Nm yr^{-1}, a value similar to what found for active plate boundaries such as California (Wenzel *et al.*, 1998). The small cloud of intermediate-depth earthquakes has been used to infer existence of a sinking, detached, piece of lithosphere at those depths (Fan *et al.*, 1998). The tight spatial clustering of the hypocenters, located in a vertical column, provides no information on the dip direction of the subduction.

6.2 *The tomographic picture*

Figure 14 shows horizontal sections, at different depths, of upper mantle structure in model PM0.5. At 100 km, the figure is dominated by a sharp change in the sign of anomaly between the lower left and the upper right halves, divided along the Tornquist-Tesseyre line (Figure 14, top left panel), a well known lineament representing the boundary between two different tectonic provinces (Zielhuis and Nolet, 1994b). The East European, cratonic, platform is characterized by faster than average velocity (blank areas correspond to gaps in data coverage), showing a relatively cool mantle below the continent. To the southwest, the Central European mantle is instead hot. Narrow, strong, seismically fast belts run below the Alps and the Dinarides. At this depth, only a rather faint fast velocity anomaly marks the Eastern Carpathians region, below the Vrancea.

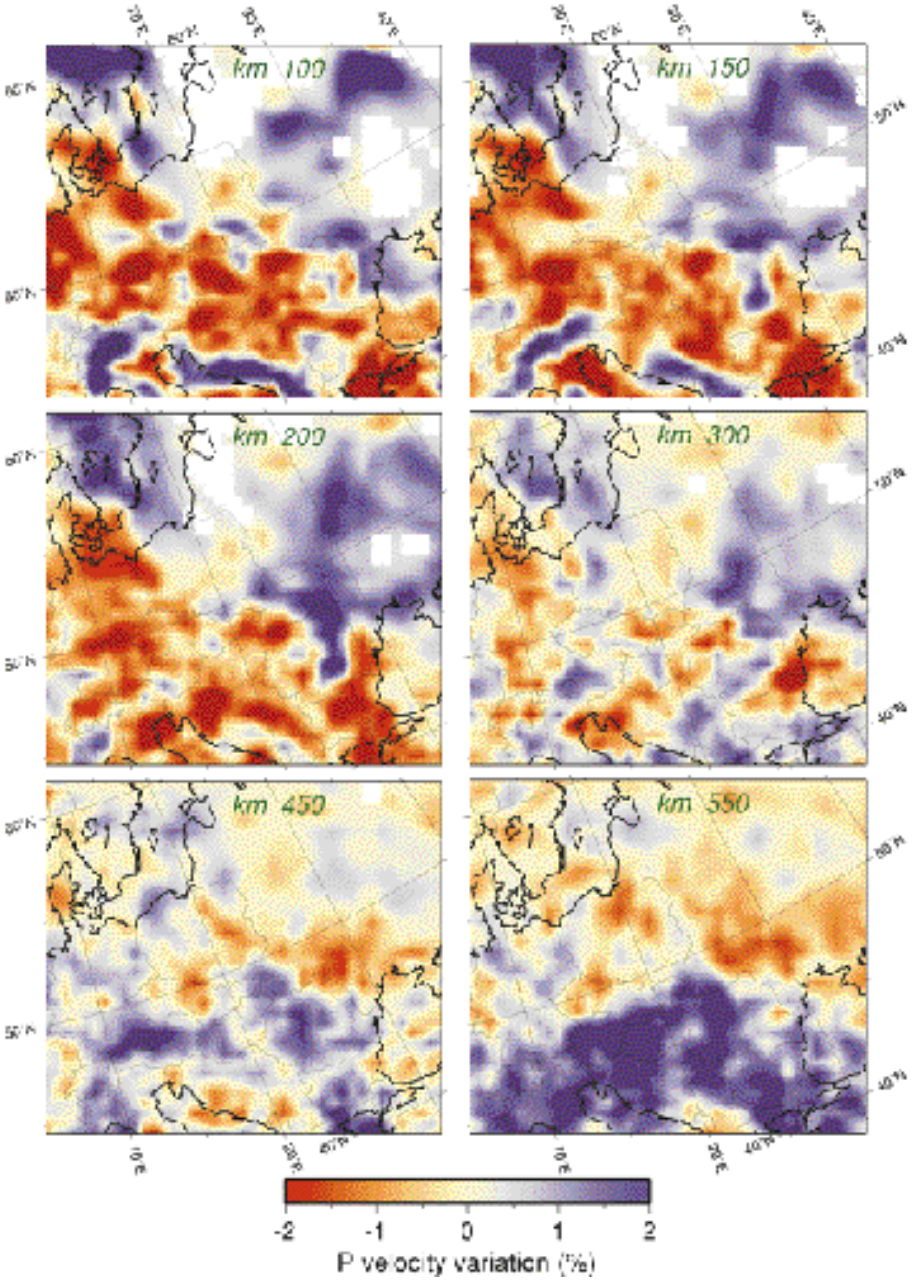

Figure 14 Maps of *P*-wave velocity variations in Northeastern Europe according to tomographic model PM0.5. Color-coded velocity representation as in Figure 3. Maps are horizontal slices cut at depths of 100, 150, 200, 300, 450, and 550 km.

The Vrancea anomaly (approximately at 46°N, 26°E) becomes well developed at larger depth, as shown by the 150 km map (Figure 14, top right). The division between the fast East European and the slow Central Europe velocities continues at this depth. The Eastern Carpathians fast anomaly corresponds to the location of intermediate-depth Vrancea earthquakes. Note that only shallow earthquakes have been used in the inversion, and therefore the significance of the association of hypocenters and fast velocities is unequivocal. The Vrancea anomaly connects to the fast velocities located across the Tornquist-Tesseyre lineament. At this depth the fast belt under the Alps is still continuous, but it is no more connected to the fast belt under the Dinarides.

At 200 km (Figure 14, center left), the main difference is the disappearance of the Dinaric and Alpine anomalies – only a small block remains below the Western Alps. Similar patterns continue at the depth of 250 km (not shown), where, however, the amplitude of the anomalies begins to decrease.

At 300 km (Figure 14, center right) the pattern changes quite dramatically. The main division between fast East European platform, and slow Central Europe has faded. Small amplitude anomalies persist. The Eastern Carpathians fast anomaly here runs to the SW, through the Balkan region. Below this depth and approaching the transition zone, anomalies decrease in amplitude and lose continuity.

A dramatically different picture characterizes the transition zone, at 450 km depth (Figure 14, bottom left). The main, outstanding, feature is a continuous fast-velocity arc, convex towards the north, running below the Western Alps, on the outer margin of the Eastern Alps, along the West Carpathians, and then bending to follow the East Carpathians. This belt corresponds to the hypothesized oceanic subduction belt, active until Eocene times, when continents began to collide (Royden and Burchfiel, 1989). Apart from this fast belt, only small-amplitude anomalies are visible.

As we go to larger depth, such as 550 km (Figure 14, bottom right), the velocity structure is rather simple. A wide aggregation of fast material is concentrated in the southernmost part of the model window, and is contrasted against another wide area that is essentially devoid of significantly strong anomalies. The fast velocity aggregate is part of the larger volume of fast material in the mantle transition zone under the center of the Mediterranean area (Figure 3).

6.3 *Comparison with other models*

The regional scale tomographic model by Spakman *et al.* (1993) shows similar features in the Carpathians region, although with less detail. A fast *P* velocity body is revealed under the belt, particularly clear between the depths of 200 and 300 and detached from shallow lithosphere.

Fan *et al.* (1998) inverted *P* and *S* travel time data originated by local shallow and intermediate-depth earthquakes and recorded by regional stations, to find a three-dimensional tomographic model of *P* and *S* wave velocity perturbations

from the surface to a depth of 200 km. At crustal depths, they found dominantly slow anomalies, associated with the lithological structure of sedimentary basins, and high velocities on the East European platform. They found low velocities along the outer arc of the Carpathians foredeep, distributed from the surface down to a depth of 70 km. This observation has been interpreted as due to subduction of continental crustal rocks. Because of the use of local data, resolution of the model diminishes with depth, and only a small region has been reliably imaged below 90 km. It shows that a high velocity body – up to +4% faster than average – exists under the Carpathians arc at depths between 100 and 170 km, outlining a slab dipping almost vertically. Intermediate-depth earthquake foci are confined within this volume. Lack of resolution at larger depth did not allow to put bounds on the bottom of this slab.

Wenzel *et al.* (1998) showed results of a high resolution tomographic study based on teleseismic observations at Romanian digital seismographic stations.

The model confirms the presence of a high velocity (+4% under Vrancea), elongated body spanning all the way from subcrustal depth to the bottom of the model (240 km). The fast body assumes a curved shape, convex to the east, but it could not be bounded laterally because of the limited geographic footprint of the seismographic network used. The fast body is surrounded by low velocities, to the east and to the west.

6.4 *Interpretation and discussion*

Unquestionable geologic evidence exists for ocean closure and continental shortening around the Carpathians arc (*e.g.*, Royden and Burchfiel, 1989; Linzer, 1996). All seismic tomographic studies agree in imaging a fast body spatially correlated with the intermediate-depth foci under the Vrancea region. This may be safely interpreted, then, as an evidence for a piece of subducted lithosphere, possibly detached from shallow lithosphere.

Details on slab extension and geometry, and its origin and nature, are however not clearly defined. The vertical dip of the slab makes it difficult to understand what the original subduction direction was, and what its possible relation was with the plate fragments involved in the complex evolution of the Pannonian-Carpathians region. Tomographic evidences agree with a kinematic model (Royden and Burchfiel, 1989; Linzer, 1996) by which retreating, westward-dipping, subduction migrated back by 600 km to open the Pannonian basin from 16 to 0.2 Ma.

It has been inferred that continental lithosphere was subducted during the development of the Pannonian-Carpathians system (*e.g.*, Royden and Burchfiel, 1989). As all oceanic terrains disappeared near the end of the Miocene, and no remnants of oceanic crust are left, it may be difficult to clarify unequivocally this issue on the basis of geologic evidence. Fan *et al.* (1998) propose that subduction initiated with oceanic lithosphere about 16 Ma, and that this leading fragment is attached to a longer slab segment of continental origin, which slowed down the

rollback velocity as it started to subduct. Existence of slow velocity anomalies surrounding the Carpathian arc at shallow depth may in fact be well explained by the presence of continental crust. On the basis of paleogeographic considerations, the continental lithosphere may be inferred to reach 180 km, and thus form the main part of the subducted slab, which can be traced down to below 200 km depth by seismicity – the deepest intermediate focal depth is 220 km – and by tomography – see Figure 14, 200 km and 300 km.

Regional-scale studies, able to reach deeper than local inversions, show that the fast anomaly continues without interruption below the maximum depth of seismicity, down to 300 km (see Figure 14; see also Spakman *et al.*, 1993). This implies that a seismically inactive slab segment exists below the active portion. However, the different shape of the fast body at 300 km and deeper – elongated and striking SW-NE in map view – suggests that a different kinematic geometry existed at the time of subduction.

Model PM0.5 shows that a significant fast structure – a long continuous curved belt, running from the Western Alps to the Eastern Carpathians – reaches the depth of 450 km (Figure 14, 450 km) and bears no geometric resemblance of the structure 150 km above. This belt may represent the oceanic lithosphere subducted by Apulian-Eurasian convergence just before differentiation between Alps and Carpathians took place before the Eocene (Royden and Burchfiel, 1989). At even greater depth (Figure 14, 550 km), cold subducted material accumulates in the transition zone in a wide a cluster.

7 Discussion

In the preceding sections, we present some characteristics of the structure of the upper mantle in the Mediterranean Africa-Eurasia collision zone outlined by travel time seismic tomography. We concentrate on a few sample regions where fast velocity anomalies image cold subducted lithosphere. The different studies mentioned agree on the larger scale signature of subduction, but do not reach a consensus on many important points. Where, for instance, is the Apenninic slab interrupted, and where is it vertically continuous? Is mantle lithosphere under the Northern Apennines delaminating, or is the slab completely detached? Is subduction responsible for the cold material present at depth under the Betic-Rif arc, or is it delaminated mantle that sunk so deep? What is the geometry and the timing of past subduction under the Carpathians? Is the cold material accumulating in the transition zone penetrating into the lower mantle? What is the exact amplitude of the velocity anomalies? The way remains open for future research to answer these and many other important questions.

In the spirit of this book, we may ask ourselves what are the factors, limiting the quality of results, which may reasonably be removed in the near (*i.e.*, foreseeable) future. Limitations of the overall amount, geographic distribution, and quality of the data are indeed prime limiting factors. Unlike exploration geophysics, large scale tomography has mostly to rely on natural sources, which are located

very inhomogeneously in space and time. Irregular geographic distribution of earthquakes induces large inhomogeneities of the density of information in the model domain, and sometimes leaves wide empty gaps. Irregular time distribution of earthquakes limits the effectiveness of temporary deployment of portable instruments. The future will certainly bring more and better data. This will not suffice to overcome the intrinsic limitations of travel time data – now the most common source of information for high resolution deep tomographic studies – and of current methods of analysis. Answers to many of the open questions will require us to extract more and better information from seismic data, by virtue of methodological improvements.

What are the goals of future improvement in the field of seismic tomography? Expectations for increased detail and sharpness of the images are natural and common. Since its inception, tomography has followed a continuous trend in reaching more and more detail. Older studies were generally limited to finding average properties of large regions (Aki *et al.*, 1977; *e.g.*, Dziewonski *et al.*, 1977) and only allowed limited tectonic or geodynamic inferences to be drawn. Dramatic improvements of computers, evolution of geophysical inverse theory, and increase of self-confidence have enabled us to retrieve models with finer and finer detail. The search for sharper images will continue understandably with more and more complex calculations.

Besides detail of tomographic models, we also need to improve the constraints on the amplitude of velocity variations. Efforts have perhaps more seldom, and less enthusiastically, been devoted to this aspect: the exact amplitude of velocity variations of a model is a subject seldom addressed by tomography scientists, who usually give more confidence to relative, rather than absolute, variations. Uncertainty in model amplitude is in fact a consequence of indetermination of this inverse problem. Nevertheless, more efforts must be devoted to the search for more correct model amplitudes, perhaps by considering different seismic data – such as surface and body waveforms – and by calibrating tomographic models with comparisons with other observations and data (see, *e.g.*, Sobolev *et al.*, 1997; Goes *et al.*, 2000).

Besides reaching more detail, and better absolute amplitude information, another goal for advancement of tomographic techniques is to improve confidence assessment. Statistics and inverse theory of course provide correct means to characterize error and resolution of a tomographic model as consequences of errors in the data and approximations introduced by the inversion. Modelling errors are much more complex to handle, and their effect on final models remains largely unknown. A detailed error assessment, based on the hypothesis of a perfect theory, leaves unsatisfactory results. Critical evaluation of modelling errors on theoretical grounds is a subject undergoing vigorous development, as testified by significant contributions given during this workshop (Nolet, 2000; Nolet and Dahlen, 2000). We need to become able to incorporate better theoretical tools to reduce simplifying assumptions, and to recognize and combine all remaining sources of uncertainty in a complete assessment of plausibility of velocity distributions resulting from inversion.

There is other information that we can, and should, use to constrain our images of deep Earth structure. We should extract more data from seismograms, such as from surface waves and from body waveforms. We should also consider knowledge deriving from other disciplines, such as geology, gravimetry, heat flow, tectonophysics, geochemistry, petrology. Their contribution is sometimes difficult to include in a quantitative way, for instance as an *a priori* constraint. This is why comparison with results of modelling other data is so important at this stage, but we need to progress on this front. Joint inversion of different geophysical quantities presents formidable difficulties but may prove to be another fundamental development to improve our picture of the Earth's deep interior.

Acknowledgements

We thank Enzo Boschi for continuing encouragement and discussion. We gratefully acknowledge constructive comments on the manuscript by Andrea Argnani and Göran Ekström. Maps have been produced using the GMT software (Wessel and Smith, 1991).

REFERENCES

AKI, K., A. CHRISTOFFERSSON and E.S. HUSEBYE (1977): Determination of the three-dimensional seismic structure of the lithosphere, *J. Geophys. Res.*, **82**, 277-296.

AMATO, A., B. ALESSANDRINI and G.B. CIMINI (1993): Teleseismic tomography of Italy, in *Seismic To - mography: Theory and Practice*, edited by H.M. IYER and K. HIRAHARA (Chapman and Hall, London), 361-396.

ARGNANI, A. (2000): The Southern Tyrrhenian subduction system: recent evolution and neotectonic implications, *Ann. Geofis.*, **43** (3), 585-607.

BIJWAARD, H. and W. SPAKMAN (2000): Non-linear global *P*-wave tomography by iterated linearized inversion, *Geophy. J.Int.*, **141**, 71-82.

BIJWAARD, H., W. SPAKMAN and E.R. ENGDAHL (1998): Closing the gap between regional and global travel time tomography, *J.Geophys.Res.*, **103**, 30055-30078.

BABUSKA, V., J. PLOMEROVA and J. SILENY (1984): Spatial variation of *P* residuals and deep structure of the European lithosphere, *Geophys. J. R.Astron. Soc.*, **79**, 363-383.

BLANCO, M.J. and W. SPAKMAN (1993): The *P*-wave velocity structure of the mantle below the Iberian Peninsula: evidence for subducted lithosphere below Southern Spain, *Tectonophysics*, **221**, 13-34.

BOSCHI, L. and A.M. DZIEWONSKI (1999): High- and low-resolution images of the Earth's mantle: implications of different approaches to tomographic modeling, *J. Geophys. Res.*, **104**, 25567-25594.

BUFORN, E., A. UDÍAS and J. MEZCUA (1988): Seismicity and focal mechanisms in South Spain, *Bull. Seismol. Soc. Am.*, **78**, 2008-2024.

BUFORN, E., A. UDÍAS, J. MEZCUA and R. MADARIAGA (1991): A deep earthquake under South Spain, 8 March 1990, *Bull. Seismol. Soc. Am.*, **81**, 1403-1407.

CALVERT, A., E. SANDVOL, D. SEBER, M. BARAZANGI, S. ROECKER, T. MOURABIT, F. VIDAL, G. ALGUACIL and N. JABOUR (2000): Geodynamic evolution of the lithosphere and upper mantle beneath the Alboran region of the Western Mediterranean: constraints from travel time tomography, *J. Geophys. Res.*, **105**, 10871-10898.

CHUNG, W.-Y. and H. KANAMORI (1976): Source process and tectonic implications of the Spanish deep-focus earthquake of March 29, 1954, *Phys. Earth Planet. Int.*, **13**, 85-96.

DAVIES, J.H. and F. VON BLANCKENBURG (1995): Slab breakoff: a model of lithosphere detachment and its test in the magmatism and deformation of collisional orogens, *Earth Planet. Sci. Lett.*, **129**, 85-102.

DERCOURT, J., L.P. ZONENSHAIN, L.-E. RICOU, V.G. KAZMIN, X. LE PICHON, A.L. KNIPPER, C. GRANDJACQUET, I.M. SBORTSHIKOV, J. GEISSANT, C. LEPVRIER, D.H. PERCHESKY, J. BOULIN, J.-C. SIBUET, L.A. SAVOSTIN, O. SOROKHTIN, M. WESTPHAL, M.L. BAZHENOV, J.P. LAUER and B. BIJU-DUVAL (1986): Geological evolution of the Tethys from the Atlantic to the Pamirs since the Lias, in *Evolution of the Tethys*, edited by J. AUBOIN, X. LE PICHON and A.S. MONIN, *Tectonophysics*, **123**, 241-315.

DEWEY, J.F., M.L. HELMAN, E. TURCO, D.H.W. HUTTON and S.D. KNOTT (1989): Kinematics of the Western Mediterranean, in *Alpine Tectonics*, edited by M.P. COWARD, D. DIETRICH and R.G. PARK, *Geol. Soc. London*, *Spec. Publ.*, **45**, 265-283.

DORREN, H.J.S. and R.K. SNIEDER (1997): Error propagation in non-linear delay-time tomography, *Geophy. J.Int.*, **128**, 632-638.

DZIEWONSKI, A.M. and D.L. ANDERSON (1981): Preliminary reference Earth model (PREM), *Phys. Earth Planet.Inter.*, **25**, 289-325.

DZIEWONSKI, A.M, B.H. HAGER and R.J. O'CONNELL (1977): Large-scale heterogeneities in the lower mantle, *J.Geophys. Res.*, **82**, 239-255.

FAN, G., T.C. WALLACE and D. ZHAO (1998): Tomographic imaging of deep velocity structure beneath the Eastern and Southern Carpathians, Romania: implications for continental collision, *J.Geophys. Res.*, **103**, 2705-2723.

GOES, S., R. GOVERS and P. VACHER (2000): Shallow mantle temperatures under Europe from *P* and *S* wave tomography, *J. Geophys. Res.*, **105**, 11153-11169.

GRAND, S.P., R.D. VAN DER HILST and S. WIDIYANTORO (1997): Global seismic tomography: a snapshot of convection in the Earth, *GSA Today*, **7**, 1-7.

GRANET, M. and J. TRAMPERT (1989): Large-scale *P*-velocity structures in the Euro-Mediterranean area, *Geophys.J.Int.*, **99**, 583-594.

GRIMISON, N.L. and W.-P. CHEN (1986): The Azores-Gibraltar plate boundary: focal mechanisms, depths of earthquakes, and their tectonic implications, *J. Geophys. Res.*, **91**, 2029-2047.

GUDMUNDSSON, O., J.H. DAVIES and R.W. CLAYTON (1990): Stochastic analysis of global travel time data: mantle heterogeneity and random errors in the ISC data, *Geophys. J. Int.*, **102**, 25-43.

HEARN, T.M. (1999): Uppermost mantle velocities and anisotropy beneath Europe, *J.Geophys. Res.*, **104**, 15123-15139.

HILL, K.C. and A.B. HAYWARD (1988): Structural constraints on the Tertiary plate tectonic evolution of Italy, *Mar. Petrol. Geol.*, **5**, 2-16.

HORVATH, F. and H. BERCKHEMER (1982): Mediterranean backarc basins, in *Alpine-Mediterranean Geodynamics*, edited by H. BERCKHEMER and K. HSU, *AGU Geodyn. Ser.*, **7**, 141-173.

HOUSEMAN, G. (1996): From mountains to basin, *Nature*, **379**, 771-772.

LE PICHON, X., F. BERGERAT and M.-J. ROULET (1988): Plate kinematics and tectonics leading to the Alpine belt formation: a new analysis, *Geol. Soc. Am.*, Special Paper 218, 111-131.

LÉVÊQUE, J.-J. and F. MASSON (1999): From ACH tomographic models to absolute velocity models, *Geophys. J. Int.*, **137**, 621-629.

LINZER, H.-G. (1996): Kinematics of retreating subduction along the Carpathians arc, Romania, *Geology*, **24**, 167-170.

LONERGAN, L. and N. WHITE (1997): Origin of the Betic-Rif mountain belt, *Tectonics*, **16**, 504-522.

LORENZ, F.P., F. WENZEL and M. POPA (1997): Teleseismic traveltime tomography of the compressional-wave velocity structure in the Vrancea zone, *Eos, Trans. Am. Geophys. Un.*, **78**, Fall Meeting Supplement, F497.

LUCENTE, F.P., C. CHIARABBA, G.B. CIMINI and D. GIARDINI (1999): Tomographic constraints on the geodynamic evolution of the Italian region, *J. Geophys.Res.*, **104**, 20307-20327.

MALINVERNO, A. and B.F. RYAN (1986): Extension in the Tyrrhenian Sea and shortening in the Apennines as result of arc migration driven by sinking of the lithosphere, *Tectonics*, **5** (2), 227-245.

MARQUERING, H. and R. SNIEDER (1996): Shear-wave velocity structure beneath Europe, the Northeastern Atlantic and Western Asia from waveform inversions including surface-wave mode coupling, *Geophy. J.Int.*, **127**, 283-304.

MELE, G., A. ROVELLI, D. SEBER and M. BARAZANGI (1996): Lateral variations of *Pn* propagation in Italy: evidence for a high-attenuation zone beneath the Apennines, *Geophys. Res. Lett.*, **23**, 709-712.

MELE, G., A. ROVELLI, D. SEBER and M. BARAZANGI (1997): Shear wave attenuation in the lithosphere beneath Italy and surrounding regions: tectonic implications, *J. Geophys. Res.*, **102**, 11863-11874.

MELE, G., A. ROVELLI, D. SEBER, T.M. HEARN and M. BARAZANGI (1998): Compressional velocity structure and anisotropy in the uppermost mantle beneath Italy and surrounding regions, *J.Geophys. Res.*, **103**, 12529-12543.

MORELLI, A. and A.M. DZIEWONSKI (1987): The harmonic expansion approach to the retrieval of deep Earth structure, in *Seismic Tomography*, edited by G. NOLET (Reidel Publishing Company, Dordrecht), 251-274.

MORELLI, A. and A.M. DZIEWONSKI (1993): Body wave travel times and a spherically symmetric *P* and *S* wave velocity model, *Geophy. J. Int.*, **112**, 178-194.

NELSON, K.D. (1992): Are crustal thickness variations in old mountain belts like the Appalachians a consequence of lithospheric delamination?, *Geology*, **20**, 498-502.

NOLET, G. (1987): Seismic wave propagation and seismic tomography, in *Seismic Tomography*, edited by G. NOLET (D. Reidel Publishing Co., Dordrecht, Holland), 1-23.

NOLET, G. (2000): Interpreting seismic waveforms: forward and inverse problems for heterogeneous media, in *Problems in Geophysics for the New Millennium,* edited by E. BOSCHI, G. EKSTRÖM and A. MORELLI, pp. 373-401 (this volume).

NOLET, G. and F.A. DAHLEN (2000): Wavefront healing and the evolution of seismic delay times, *J. Geophys. Res.* (in press).

PAIGE, C.C. and M.A. SAUNDERS (1982): LSQR: an algorithm for sparse linear equations and sparse least squares, *ACM Trans. Math. Softw.*, **8**, 43-71.

PATACCA, E., R. SARTORI and P. SCANDONE (1993): Tyrrhenian basin and Apennines: kinematic evolution and related dynamic constraints, in *Recent Evolution and Seismicity of the Mediterranean Region*, edited by E. BOSCHI, E. MANTOVANI and A. MORELLI, NATO ASI Series (Kluwer, Dordrecht), 161-171.

PIROMALLO, C. and A. MORELLI (1997): Imaging the Mediterranean upper mantle by *P*-wave travel time tomography, *Ann. Geofis.*, **40** (4), 963-979.

PIROMALLO, C. and A. MORELLI (1998): *P*-wave propagation heterogeneity and earthquake location in the Mediterranean region, *Geophys. J. Int.*, **135**, 232-254.

PIROMALLO, C. and A. MORELLI (2000a): Improving seismic event location: an alternative to three-dimensional structural models, *Pure Appl. Geophys.* (in press).

PIROMALLO, C. and A. MORELLI (2000b): Seismic travel time tomography of Mediterranean, European and Middle Eastern upper mantle and transition zone (in preparation).

ROMANOWICZ, B. (1980): A study of the large-scale lateral variations of *P* velocity in the upper mantle beneath Western Europe, *Geophys. J. R. Astron. Soc.*, **63**, 217-232.

REUTTER, K.-J., P. GIESE and H. CLOSS (1980): Lithospheric split in the descending plate: observations from the Northern Apennines, *Tectonophysics*, **64**, T1-T9.

ROYDEN, L. and B.C. BURCHFIEL (1989): Are systematic variations in thrust belt style related to plate boundary processes? (the Western Alps *versus* the Carpathians), *Tectonics*, **8**, 51-61.

SAGNOTTI, L., A. WINKLER, P. MONTONE, L. DI BELLA, F. FLORINDO, M.T. MARIUCCI, F. MARRA, L. ALFONSI and A. FREPOLI (1999): Magnetic anisotropy of Plio-Pleistocene sediments from the Adriatic margin of the Northern Apennines (Italy): implications for the space-time evolution of the stress field, *Tectonophysics*, **311**, 139-153.

SEBER, D., M. BARAZANGI, A. IBENBRAHIM and A. DEMNATI (1996a): Geophysical evidence for lithospheric delamination beneath the Alboran Sea and the Betic-Rif mountains, *Nature*, **379**, 785-790.

SEBER, D., M. BARAZANGI, B.A. TADILI, M. RAMDANI, A. IBENBRAHIM and D. BEN SARI (1996b): Three-dimensional upper mantle structure beneath the intraplate Atlas and interplate Rif mountains of Morocco, *J.Geophys.Res.*, **101**, 3125-3138.

ŞENGÖR, A.M.C. (1993): Some current problems on the tectonic evolution of the Mediterranean during the Cenozoic, in *Recent Evolution and Seismicity of the Mediterranean Region*, edited by E. BOSCHI, E. MANTOVANI and A. MORELLI, NATO ASI Series (Kluwer, Dordrecht), 1-51.

SERRI, G., F. INNOCENTI and P. MANETTI (1993): Geochemical and petrological evidence of the subduction of delaminated Adriatic continental lithosphere in the genesis of the Neogene-Quaternary magmatism of Central Italy, *Tectonophysics*, **223**, 117-147.

SNIEDER, R. (1988): Large-scale waveform inversions of surface waves for lateral heterogeneity, 2, application to surface waves in Europe and the Mediterranean, *J. Geophys. Res.*, **93**, 12067-12080.

SOBOLEV, S.V., H. ZEYEN, M. GRANET, U. ACHAUER, C. BAUER, F. WERLING, R. ALTHERR and K. FUCHS (1997): Upper mantle temperatures and lithosphere-asthenosphere system beneath the French Massif Central constrained by seismic, gravity, petrologic and thermal observations, *Tectono - physics*, **275**, 143-164.

SPAKMAN, W. (1991): Delay time tomography of the upper mantle below Europe, the Mediterranean and Asia Minor, *Geophy. J.Int.*, **107**, 307-332.

SPAKMAN, W., S. VAN DER LEE and R. VAN DER HILST (1993): Travel-time tomography of the European-Mediterranean mantle down to 1400 km, *Phys. Earth Planet.Inter.*, **79**, 3-74.

UDIAS, A., A. LOPEZ ARROYO and J. MEZCUA (1976): Seismotectonics of the Azores-Alboran region, *Tectonophysics*, **31**, 259-289.

VAN DER HILST, R., S. WIDIYANTORO and E.R. ENGDAHL (1997): Evidence for deep mantle circulation from global tomography, *Nature*, **386**, 578-584.

VAN DER MEULEN, M.J., J.E. MEULENKAMP and M.J.R. WORTEL (1998): Lateral shifts of Apenninic fore-deep depocentres reflecting detachment of subducted lithosphere, *Earth Planet. Sci. Lett.*, **154**, 203-219.

WENZEL, F., U. ACHAUER, D. ENESCU, E. KISSLING, R. RUSSO, V. MOCANU and G. MUSACCHIO (1998): Detailed look at final stage of plate break-off is target of study in Romania, *Eos, Trans.Am. Geophys. Un.*, **48**, 589-594.

WESSEL, P. and W.H.F. SMITH (1991): Free software helps map and display data, *Eos, Trans. Am.Geo - phys. Un.*, **72**, 445-446.

WESTAWAY, R. (1993): Quaternary uplift of Southern Italy, *J.Geophys. Res.*, **98**, 21741-21772.

WORTEL, M.J.R. and W. SPAKMAN (1992): Structure and dynamics of subducted lithosphere in the Mediterranean region, *Proc. K. Ned. Akad. Wet.*, **95**, 325-347.

ZIELHUIS, A. and G. NOLET (1994a): Shear-wave velocity variations in the upper mantle beneath Central Europe, *Geophy. J. Int.*, **117**, 695-715.

ZIELHUIS, A. and G. NOLET (1994b): Deep seismic expression of an ancient plate boundary in Europe, *Science*, **265**, 79-81.